Journal of Umm Al-Qura University for Applied Sciences
https://doi.org/10.1007/s43994-024-00135-z

REVIEW

The early Danian event (Dan-C2) and the latest Danian event (LDE): a case study from Gebel Kilabiya, Egypt

Orabi H. Orabi[1] · Heba Ismail[2] · Saida Taha[3]

Received: 21 September 2023 / Accepted: 10 February 2024

Abstract
At the Gebel Kilabiya area, studies on foraminifera and isotopes were conducted during the Paleocene. The data revealed that the lowest part of the P2 Zone and the oldest peak, P1c, closely resemble the Dan-C2 event. Before Dan-C2, the diversity of the assemblages rapidly declined as the abundance of the agglutinant *Spiroplectinella spectabilis*, and calcareous benthic *Bulimina* spp., species commonly known as an opportunist, increased may be influenced by warmth and pH changes due to Deccan volcanism. The extinction of the planktic foraminifera genus *Praemurica* occurred shortly before the Latest Danian Event (LDE). Additionally, praemuricids were eventually supplanted by morozovellids in parallel. Warm morphogroups *Praemurica*, *Morozovella, Igorina,* and *Acarinina* are found in the low latitude group; they show a tendency towards warming in the late Paleocene (Zone P3a and P3b).

Keywords Foraminifera · Dan-C2 event · Epifaunal · Infaunal · Latest Danian Event · Gebel Kilabiya

1 Introduction

A sequence of brief warming episodes known as "hyperthermals" interrupted the early Paleogene greenhouse expertise (Bornemann et al. 2009; Westerhold et al. 2018, 2020), [1–3]. In marine ecosystems, these hyperthermals exhibit accelerated sea-floor carbonate disintegration, deep-to-intermediate water oxygen depletion, and temporary alterations in marine benthic fauna. They also have a negative carbon isotope excursion (CIE). Those characteristics point to the significant input of 13C-depleted carbon from an external carbon store to the ocean–atmosphere system, which raised temperature and pCO2 levels in the atmosphere. These episodes involved (i) the early Danian Dan-C2 event (~65.2 Ma) [4, 5]; (ii) the Latest Danian Event (~61.7 Ma) [5]; (iii) the Mid Paleocene Biotic Event (MPBE) (~58.2 Ma) is sometimes referred to as the Early-Late Paleocene Event (ELPE) [6, 7], and (iv) the Thermal Maximas 2 and 3 of the early Eocene (~53.7 and ~53.6 Ma, 34 respectively) [8].

In the last 10 years, evidence of a warming episode with a 200-thousand-year time scale has been found in some oceanic and shallow marine basins [5, 8–10]. According to data from deep-sea deposits, the LDE is characterized by the decrease in sedimentary CaCO3, additionally negative $\delta^{13}C$ and $\delta^{18}O$ excursions in benthic and planktic foraminiferal calcite [11–13]. According to estimations of the temperature of oxygen isotopes, during the LDE, the water is often warmed by 2–3 °C [14]. Also, Schulte et al. [15] showed that the LDE is connected to carbonate-poor sediments in the Qreiya 3 region (Egyptian shelf).

Over the past few years, in the deep sea and on regions of the shelf, some research has concentrated on the detection of LDE and the benthic reaction [16–19]. Data on planktic ecosystems in the open ocean have been scarce up to this study [20, 21]. Conversely, more regular investigations from the Tunisian and Egyptian shelves are often limited by the absence of a precise stratigraphic basis.

In this study, we provide a comprehensive analysis of the planktic foraminiferal assemblage information using a quantitative approach, and we assess the supra-regional response of the marine planktic ecosystem to the LDE. This study

✉ Orabi H. Orabi
Oraby1952@yahoo.com

[1] Geology Department, Faculty of Science, Menoufia University, Shiben El Kom, Egypt

[2] Department of Geology, Faculty of Science, Alexandria University, Alexandria 21568, Egypt

[3] Department of Petroleum Geology, Faculty of Petroleum and Mining Science, Matrouh University, Marsa Matrouh, Egypt

Published online: 25 March 2024

also includes new data from Egypt's southern Tethyan shelf, which is based on two South Atlantic recordings that were previously published [14, 22]. The Tethyan shelf section's well-dated combination offers a preliminary broad picture of alterations in the planktic foraminiferal assemblage that accompanied the LDE in Egypt.

This study will evaluate the benthic foraminiferal turnover in the Kilabiya area to examine how the fauna and paleoenvironment responded to the Dan-C2 event, which happened subsequent to the Cretaceous/Paleogene (K/Pg) boundary (Fig. 1). For the LED in the Kilabiya section, we reported the first planktic foraminiferal data at high resolution. To monitor the paleoenvironmental and faunal reaction, we investigated the planktic foraminiferal turnover.

2 Geological setting and lithostratigraphy

Egypt's shelf region is separated into the Unstable Shelf and the Stable Shelf encircling the Arabo-Nubian craton in the Late Cretaceous and Early Paleogene [30]. During the Campanian-Paleocene, the study location was situated on the northwest margin of the Arabian-Nubian massif, on a broad epicontinental shelf near the southern edge of the Tethys Ocean [23]. The distribution and thicknesses of facies were greatly complicated vertically and laterally as a result of tectonic control of the Egyptian Campanian-Paleocene depositional settings [24, 25].

Kilabiya area is located adjacent to the village of Kilabiya, 10 km west of Gebel Owaina, 42 km south of Luxor, and ~ 30 km north of Esna. It is located at Latitude: 25° 17′ 11″ N and Longitude: 32° 42′ 17″ E (Fig. 1).

About 19 m in the Dakhla Formation (Danian to lower Selandian), are where we collected our samples. The bulk of the almost 70 m-thick layers of the Dakhla Formation and consist of shale, green, and light grey at the lower and upper parts respectively, and marl bands. Late Maastrichtian–Middle Paleocene was the age assigned [26].

The two lithological members of the Dakhla Formation are the members of the Sharawna and Lower Owaina shale [27]. The base of the Owaina Shale Member is composed of clay ironstone bands as well as greenish grey, dark grey, greenish violet, and greenish-yellow sandstones. There is intercalation of gypsum veins, notably in the bottom half.

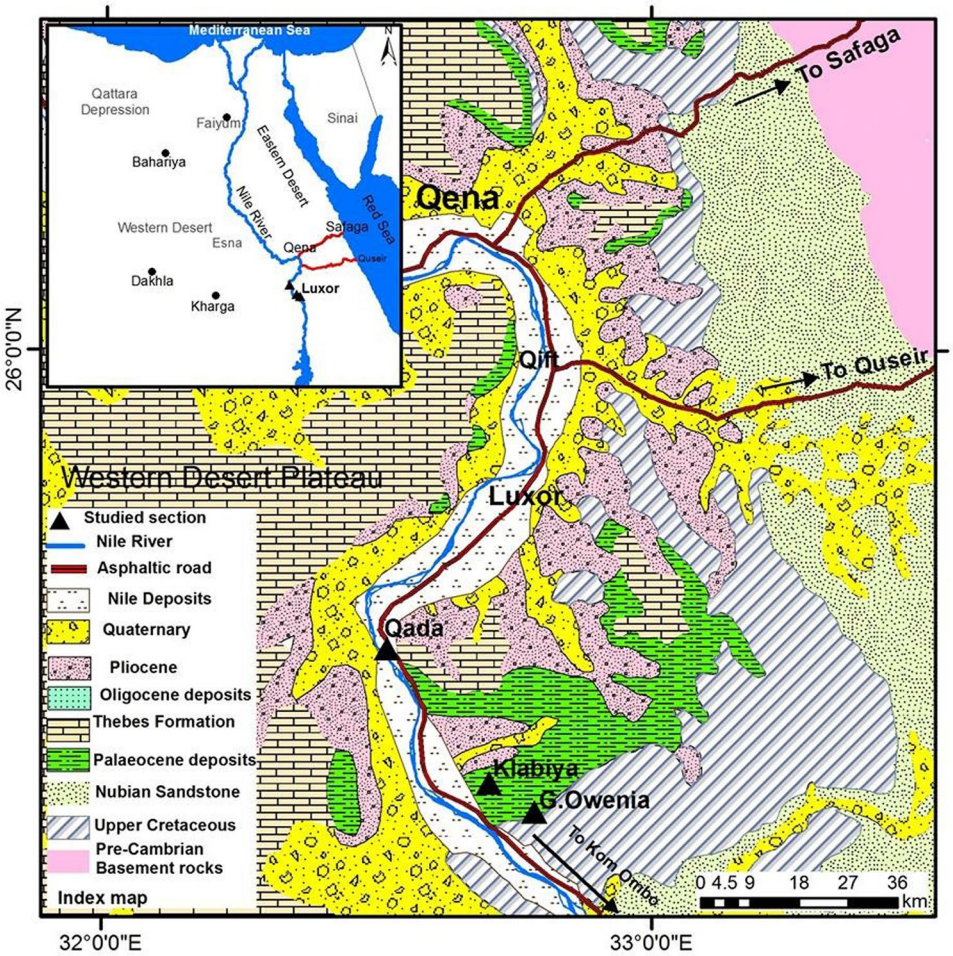

Fig. 1 Location map (modified after Geological map of Egypt, 1981) [91]

The lower Owaina Shale Member's surface is located near the well-known disconformity between the Cretaceous and Paleocene (Fig. 2). The upper part of this member is about 9.75 m thick and consists of light grey to pale greenish grey shales, calcareous shales, and dark grey clay intercalated with gypsum and has pelecypod.

Lithologically, the Dakhla Formation is equivalent to the Esna Formation of [22], the Dakhla Formation of Said (1962) [23]; the lower part of the Esna group of [27], and the Dakhla Formation of [28] and [29] (Table 1).

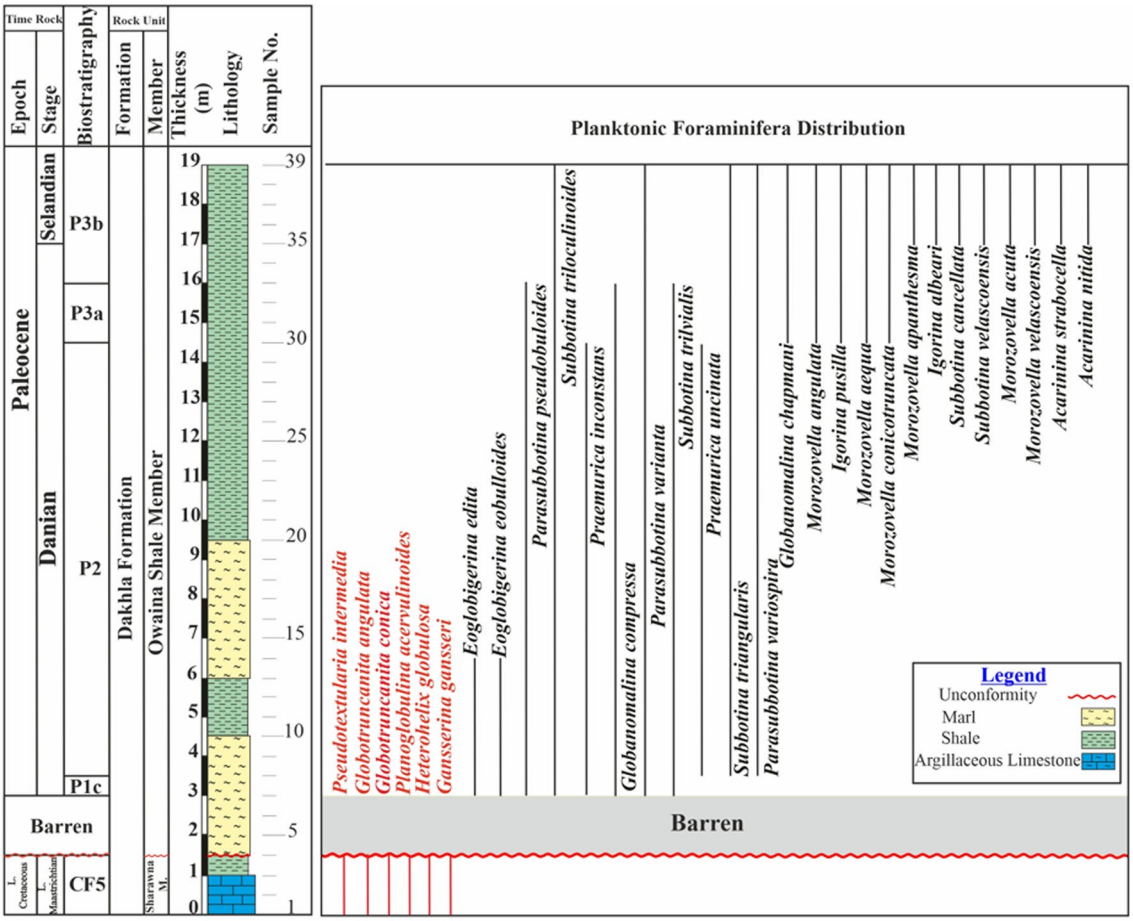

Fig. 2 Range chart of the identified planktic foraminifera in the studied section

Table 1 Correlation of the recorded Paleocene planktic foraminiferal zones with their equivalents in Egypt

Epoch	Stage	Biozone	El Naggar (1966)	Faris et al. (1985)	Obaidallah (2013)	El Younsy (2017)	El-Baz (2020)	Present study
Paleocene	Danian	P3b	*Pusilla*	*Pusilla Pusilla*	*albeari/carinata*	*Albeari/carinata*	*Albeari/pseudom-enardii*	*Albeari*
		P3a	*Uncinata*	*Angulata*	*angulata*	*Angulata*	*Angulate/ albeari*	*Pusilla*
		P2		*Uncinata*	*uncinata*	*Uncinata*	*uncinata*	*Uncinata*
		P1c	*Compressa/ Doubjergensis*	Trinidad-ensis	*inconstans*	*Inconstans*	*inconstans*	*Compressa*
		P1b			*triloculinoides*	*Triloculinoides*	*triloculinoides*	Hiatus
		P1a			*pseudobulloides*	*Pseudobulloides*	*pseudobulloides*	
		Pα	Hiatus		*eugubina*	*Eugubina*	Hiatus	
		P0				*Cretacea*		

3 Material and methods

3.1 Foraminifera studies

All of the samples were dried in an oven set at 60 °C for at least 24 h. Each sample weighed 50 gm. It was then soaked in a 10% hydrogen peroxide solution, rinsed > 63 µm, dried, and sieved throw fractions > 250, 125, and 63 mesh to extract clean fossils. The fraction 63 µm was chosen because it is thought to be the most suitable for studying the benthic and planktic community. Under a binocular microscope at a magnification of 50 X, planktic foraminifera tests were recognized using the taxonomic theories of [30–32].

The statistics calculated included the Total Foraminifera Number (TFN), Benthic Foraminifera Number (BNF), Planktic Foraminifera Number (PFN), Planktic Percent, or Oceanity Index (P%).

Gibson, (1989) [33] measures the total percent of the planktic forms relative to the total number of individual foraminifera in the sample as follows: P% = P/ (P + B) X 100, where P = the number of planktic foraminifera and B = the number of benthic foraminifera. Parameters calculation also include Infaunal % **(Inf %)**, Epifaunal percent **(Epi %)**, and **simple diversity** = the number of species per sample. The Calcareous/Arenaceous benthic ratio **(C/A)** is an important tool for determining the paleo depth. The Calcareous/Arenaceous ratio (C/A = C/C + A × 100), where C = calcareous benthic foraminifera and A = arenaceous benthic foraminifera. These parameters and the Dan-C2 as well as the LDE are shown in Fig. 3.

Planktic foraminifera from the Kilabiya section have sparse overgrowth and early signs of recrystallization, but overall there is moderate to good preservation, according to light and scanning electron microscopy examinations. At Alexandria University, scanning electron microscopic (JEOL JSM-5500 LV) is used to take pictures of the most significant planktic foraminifera (Figs. 4567).

3.2 Cluster analysis

Cluster analysis is applied to benthic foraminifera's relative frequency data in this section. The statistical analysis is performed using the "Minitab" and the species with a relative frequency of 5% are excluded.

3.3 Stable isotope analyses

Analysis of stable isotopes was done in the IAMC-CNR Institute of Naples using a Thermo Electron Delta Plus XP mass spectrometer and an automated continuous-flow carbonate preparation Gas Bench II system. Samples were acidified at a temperature of 50 °C. Every thirty samples were evaluated against the NBS19, and every six samples were compared to Carrara Marble, with δ18O = 2.43 versus

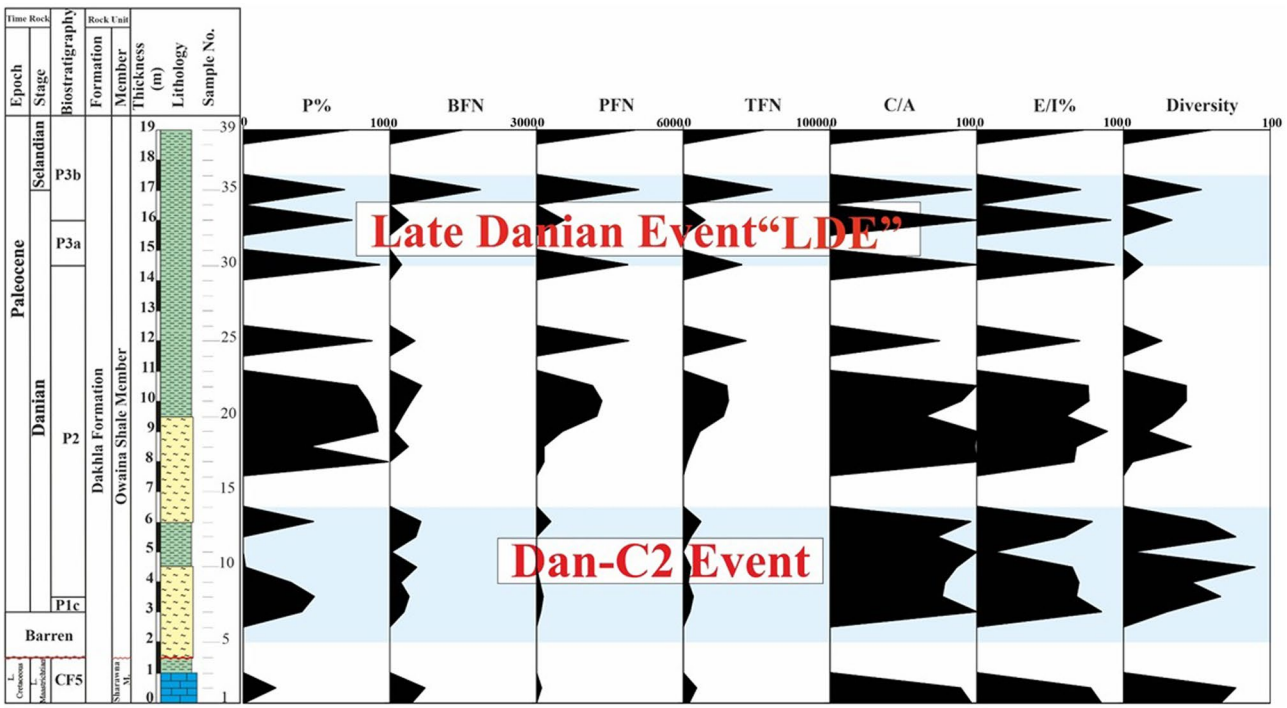

Fig. 3 The foraminifera parameters are calculated at the Early Danian Event (Dan-C2) and the Latest Danian Event (LDE)

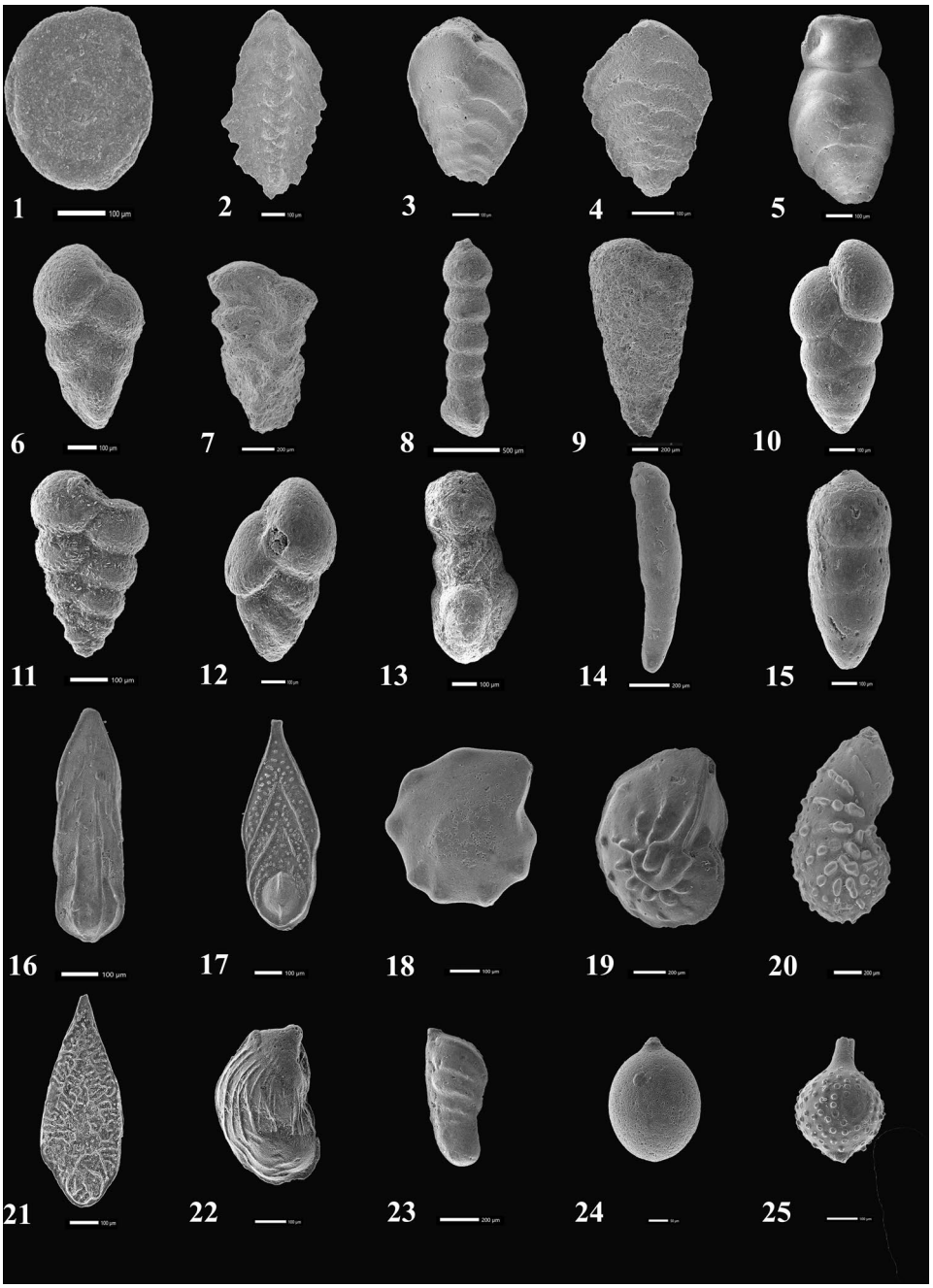

Fig. 4 Benthic foraminifera chosen by scanning electron microscope images (scale bar 100 m). 1 *Ammodiscus cretaceous* (Reuss), sample 20, P2 Zone, Kilabiya section. 2 *Spiroplectinella dentate* (Alth), sample 24, P2 Zone, Kilabiya section. 3 *Spiroplectinella esnaensis* (Le Roy), sample 24, P2 Zone, Kilabiya section. 4 *Spiroplectinella henryi* (LeRoy), sample 25, P2 Zone, Kilabiya section. 5 *Vulvulina colei* (Cushman), sample 27, P2 Zone, Kilabiya section. 6 *Gaudryina aissina* (Ten Dam and Sigal), sample 27, P2 Zone, Kilabiya section. 7 *Gaudryina nekhlensis* (Said and Kenawy), sample 26, P2 Zone, Kilabiya section. 8 *Tritaxia midwayensis* (Cushman), sample 27, P2 Zone, Kilabiya section. 9 *Dorothia oxycana* (Reuss), sample 29, P2 Zone, Kilabiya section. 10 *Marssonella indentata* (Cushman and Jarvis), sample 27, P2 Zone, Kilabiya section. 11 *Textularia farafraensis* (Le Roy), sample 27, P2 Zone, Kilabiya section. 12 *Textularia schwageri* (LeRoy), sample 28, P2 Zone, Kilabiya section. 13 *Psuedoclavulina clavata* (Cushman), sample 28, P2 Zone, Kilabiya section. 14 *Laevidentalina colei* (Cushman and Dusenbury), sample 28, P2 Zone, Kilabiya section. 15 *Pseudonodosaria manifesta* (Reuss), sample 7, P1c Subzones, Kilabiya section. 16 *Frondicularia archiaciana* (D'Orbigny), sample 25, P2 Zone, Kilabiya section. 17 *Frondicularia frankei* (Cushman), sample 32, P3a Subzone, Kilabiya section. 18- *Lenticulina* sp1, sample 25, P2 Zone, Kilabiya section, 19- *Lenticulina* sp 2, sample 24, P2 Subzone, Kilabiya section. 20 *Marginulinopsis tuberculata* (Plummer), sample 26, P2 Zone, Kilabiya section. 21 *Neoflabellina semireticulata* (Cushman and Jarvis), sample 32, P3a Subzone, Kilabiya section. 22 *Marginulina carri* (Le Roy), sample 22, P2 Zone, Kilabiya section. 23 *Vaginulina cretacea* (Plummer), sample 24, P2 Zone, Kilabiya section. 24 *Lagena apiculata* (Reuss), sample 25, P2 Zone, Kilabiya section. 25 *Lagena hispida* (Reuss), sample 31, P3a Subzone, Kilabiya section

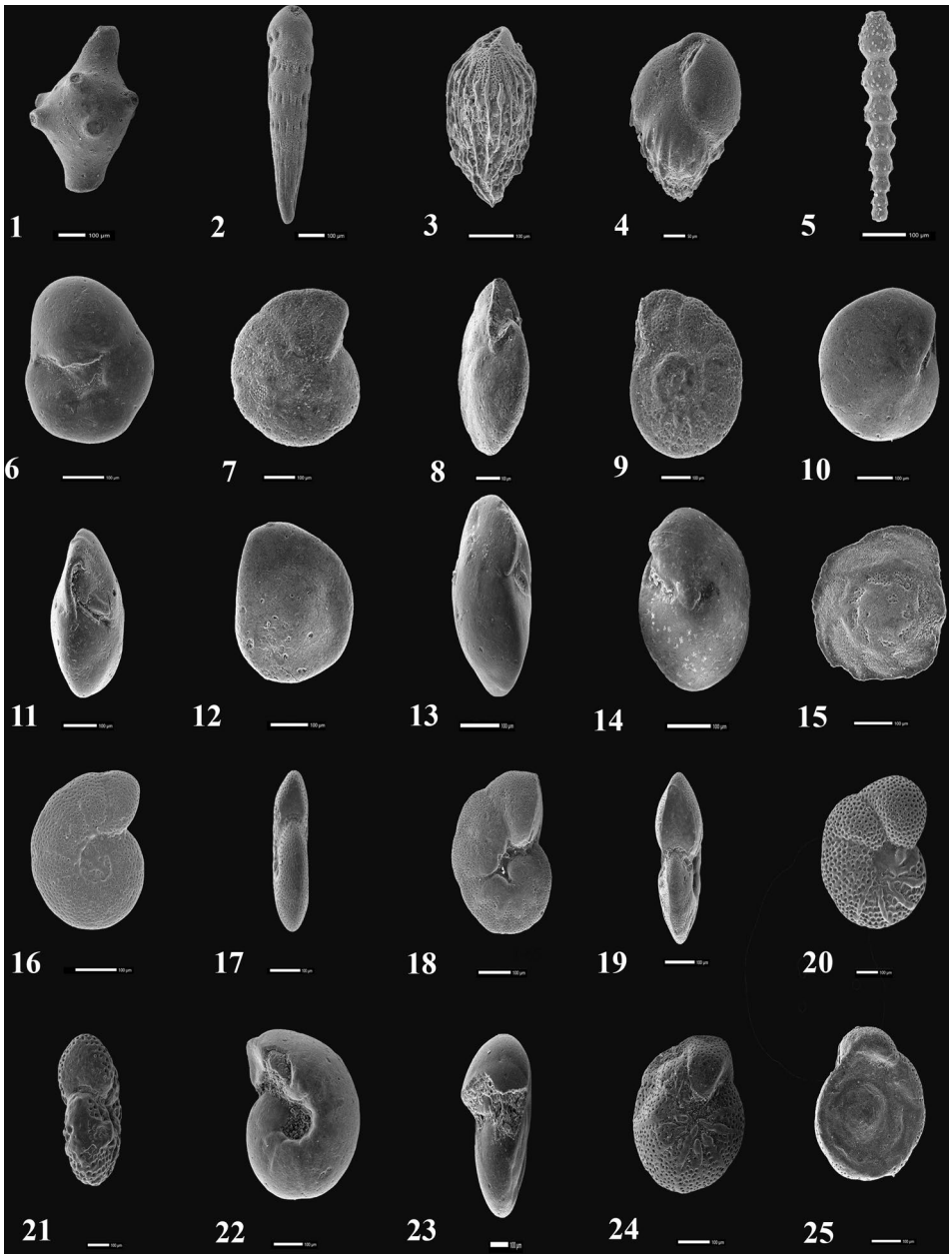

Fig. 5 Benthic foraminifera chosen by scanning electron microscope images (scale bar 100 m). 1 *Ramulina navarroana* (Cushman), sample 24, P2 Zone, Kilabiya section. 2 *Loxostomoides applinae* (Plummer), sample 23, P2 Zone, Kilabiya section. 3 *Bulimina farafraensis* (Le Roy), sample 22, P2 Subzone, Kilabiya section. 4 *Bulimina midwayensis* (Cushman and Parker), sample 27, P2 Zone, Kilabiya section. 5 *Stilostomella paleocenica* (Cushman and Todd), sample 25, P2 Zone, Kilabiya section. 6 *Cancris auricula* (Fichtel and Moill), sample 32, P3a Subzone, Kilabiya section. 7–9 *Cibicidoides pseudoacutus* (Nakkady), 7- umbilical view, 8- lateral view with aperture, 9- spiral view, sample 25, P2 Zone, Kilabiya section. 10–12 *Alabamina midwayensis* (Brotzen); 10- umbilical view, 11- lateral view with aperture, 12- spiral view, sample 28, P2 Zone, Kilabiya section. 13,14 *Oridosalis plummerae* (Cushman); 15- spiral view, 16- umbilical view, sample 27, P2 Zone, Kilabiya section. 15 *Osangularia plummerae* (Brotzen); sample 22, P2 Zone, Kilabiya section; 16,17 *Anomalinoides affinis* (Hantken); sample 32, P3a Subzone, Kilabiya section. 18, 19 *Anomalinoides praeacutus* (Vasilenko); sample 7, P1c Subzones, Kilabiya section. 20, 21 *Gavelinella rubiginosa* (Cushman); sample 25, P2 Zone, Kilabiya section. 22, 23 *Gyroidinoides girardanus* (Reuss); 22- umbilical view; 23- lateral view with aperture, sample 32, P3a Subzone, Kilabiya section. 24, 25 *Angulogavelinella avnimelechi* (Reiss), 24- umbilical view; 25- lateral view with aperture, sample 32, P3a Subzone, Kilabiya section

Vienna Pee Dee Belemnite [VPDB] and δ13C = 2.43 versus VPDB. Based on repeat measurements taken from 20% of the analyzed samples, the standard deviations of carbon

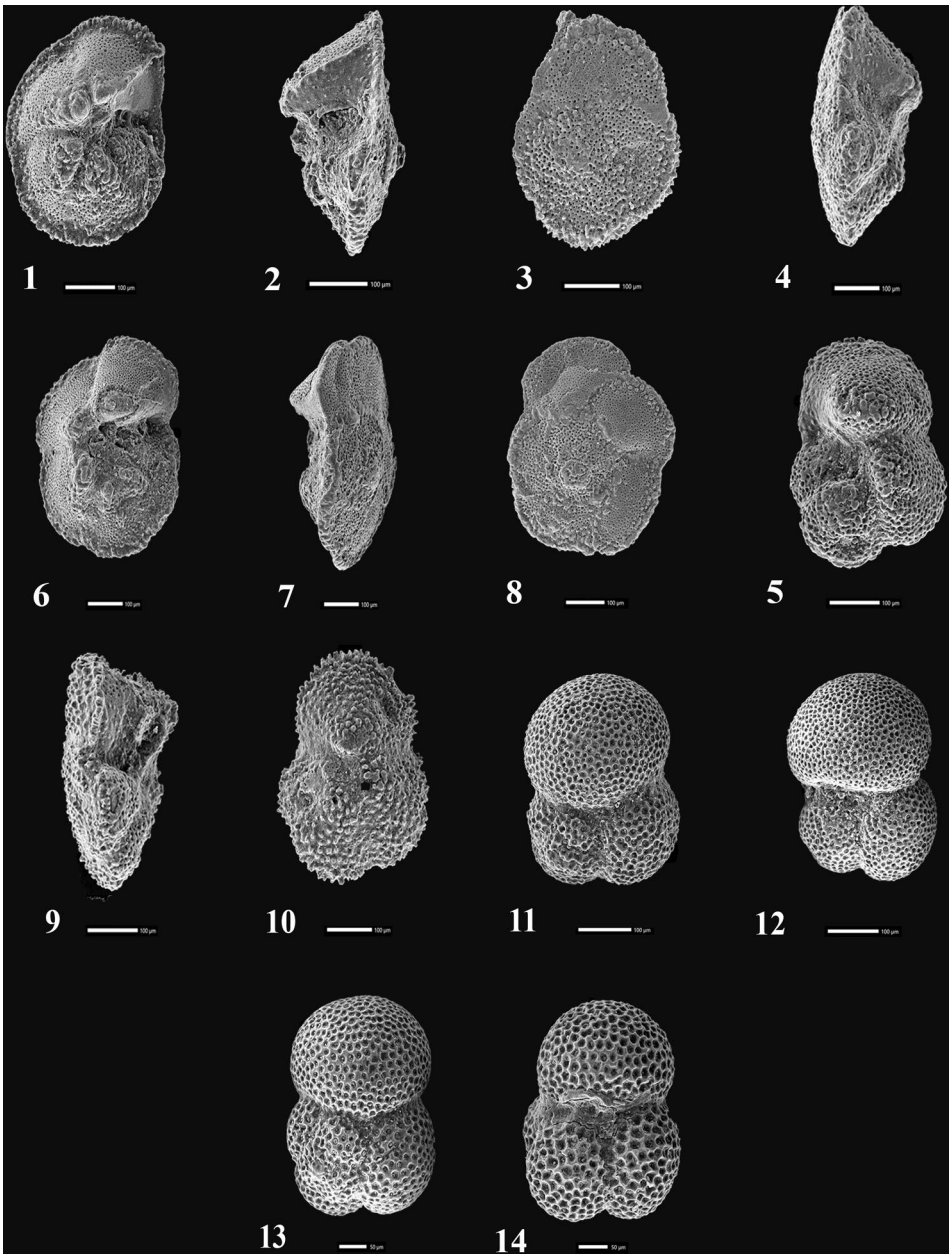

Fig. 6 photos taken with a scanning electron microscope of particular planktic foraminifera (Scale bar is 100 µm). 1–3 *Morozovella acuta* (Toulmin); 1- umbilical view, 2- lateral view with aperture, 3- spiral view, sample 35, P3b Subzone, Kilabiya section. 4,5 *Morozovella aequa* (Cushman and Renz); 4- lateral view with aperture; 5- umbilical view; sample 32, P3a Subzone, Kilabiya section. 6–8 *Morozovella angulata* (White); 6- umbilical view; 7- lateral view with aperture; 8- spiral view; sample 31, P3a Subzone, Kilabiya section. 9,10 *Morozovella subbotinae* (Morozova); 9- lateral view with aperture; 10- umbilical view, samples 42, 43, P4a Subzone, Kilabiya section. 11, 12 *Subbotina triloculinoides* (Plummer); 11- spiral view; 12- umbilical view; sample 35, P3b Subzone, Kilabiya section. 13, 14 *Subbotina velascoensis* (Cushman); 13- umbilical view; 14- spiral view; sample 18, P2 Zone, Kilabiya section

and oxygen isotope readings were calculated to be 0.1 and 0.08‰.

From the 125–180 µm size fraction, three to seven *Nuttallides truempyi* specimens were chosen for stable isotope studies of benthic foraminifera. All of the samples were exposed to 100% phosphoric acid at 75 °C using a Kiel IV to a MAT 253 mass spectrometer (University Leipzig). Analysis from the Qreiya 3 area of Egypt was used to compare samples of the benthic *Pyramidulina* [15] (Fig. 8), and samples at the University of Erlangen utilizing a Kiel III online carbonate preparation line linked to a Thermo Finnigan 252 mass spectrometer. Reproducibility was tested, and for both $\delta^{13}C$ and $\delta^{18}O$, it was consistently better than ± 0.1‰ (1σ).

4 Biostratigraphy

The biozonation criteria of [30] and [32] were used to apply the planktic foraminifer biostratigraphy [34]. Planktic foraminifera Zones P1, P2, and P3 include the majority of the study interval (Fig. 2). The P1/P2 and P2/P3 Zonal boundaries are determined by the Lowest Occurrences (LO) of *Praemurica uncinata* and *Morozovella angulata*, respectively. *Globanomalina pseudomenardii* is a common and large species [31]. *Globanomalina* specimens (125 µm) are referred to as *G. pseudomenardii,* and their LO is indicated. Our current research focuses on the biozones P1c, P2, and P3a.

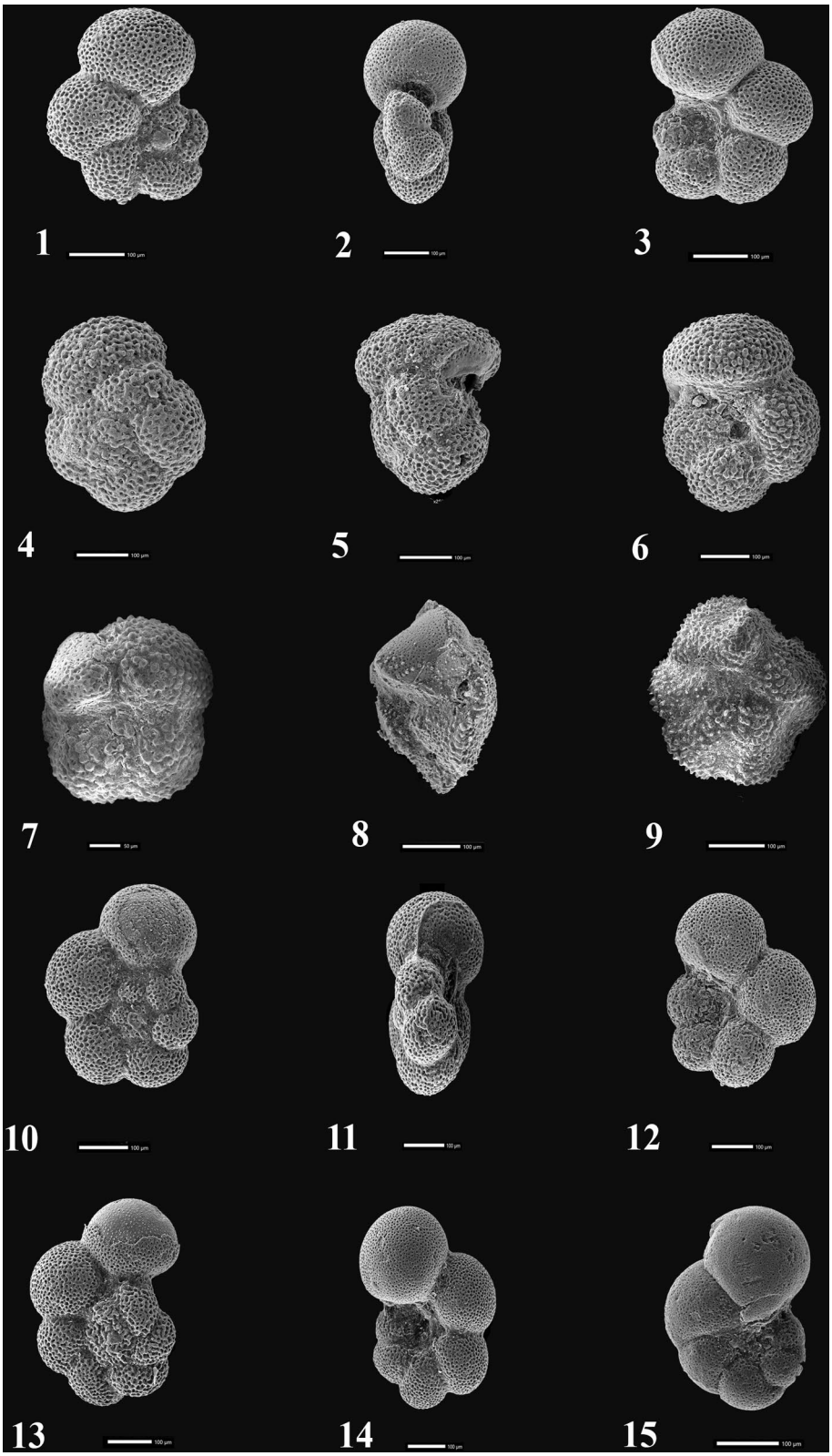

Fig. 7 photos taken with a scanning electron microscope of particular planktic foraminifera (Scale bar is 100 µm). 1–3 *Parasubbotina pseudobulloides* (Plummer); 1- spiral view, 2- lateral view with aperture, 3- umbilical view, sample 19, P2 Zone, Kilabiya section. 4–6 *Acarinina soldadoensis* (Brönnimann); 4- spiral view, 5- lateral view with aperture, 6- umbilical view, sample 39, P3b Subzone, Kilabiya section. 7 *Acarinina wheti* (Weiss); umbilical view, sample 38, P3b Subzone, Kilabiya section. 8, 9 *Igorina pusilla* (Bolli), 8- lateral view with aperture, 9- umbilical view, sample 32, P3a Subzone, Kilabiya section. 10–12 *Praemurica inconstans* (Subbotina); 12- spiral view; 13- lateral view with aperture; 14- umbilical view; sample 16, P2 Zone, Kilabiya section. 13,14 *Praemurica uncinata* (Bolli); 13- spiral view; 14- umbilical view; sample 16, P2 Zone, Kilabiya section. 15 *Globanomalina pseudomenardii* (Bolli); sample 39, P3b Subzone, Kilabiya section

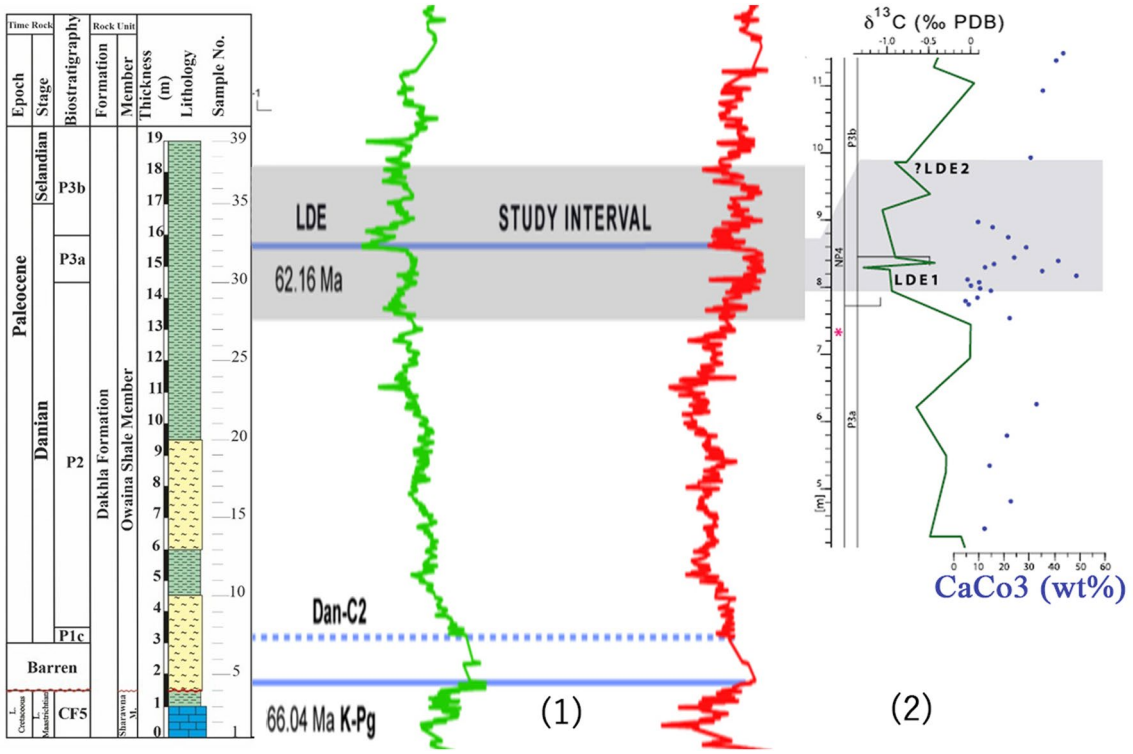

Fig. 8 Dendrogram resulting from the cluster analysis of benthic foraminifera in the Kilabiya section

4.1 Zone P1. *Eoglobigerina edita* partial-range zone

Author: Berggren et al. (1995) [35].

Definition: The nominate taxon lies between Praemurica uncinata's LO and Parvularugoglobigerina eugubina's highest occurrence (HO).

Estimated age: early Paleocene.

4.1.1 Subzone P1c

Lowest-occurrence Subzone of *Globanomalina compressa* (therefore modified and renamed Subzone P1c of Berggren and Pearson, 2005 [30] is the lowest-occurrence subzone of *Galamalina compressa/Praemurica inconstans*; = Subzone P1c of Berggren and Pearson, 2005 [30] is the *Galamalina compressa/Praemurica inconstans–Praemurica uncinata* Subzone.

Definition: Interval of biostratigraphy exists between Globanomalina compressa and Praemurica uncinata LOs.

Estimated age: early Paleocene.

Occurrence: At the Gebel Kilabiya section (Fig. 2), it reaches a thickness of approximately 0.5 m (samples 7–8).

4.2 Zone P2. *Praemurica uncinata* lowest-occurrence zone

Author: Berggren et al. (1995) [35].

Definition: The biostratigraphic interval that exists between *Morozovella angulata*'s and *Praemurica uncinata*'s LO.

Estimated age: early Paleocene (late Danian).

Occurrence: It attains a thickness of about 11 m (samples 9 to 30) (Fig. 2).

4.3 Zone P3. *Morozovella angulata* Lowest-occurrence Zone

Author: Berggren et al. (1995([35].

Definition: The biostratigraphic interval exists between *Globanomalina pseudomenardii*'s and *Morozovella angulata*'s LO.

Estimated age: early–middle Paleocene.

4.3.1 Subzone P3a. *Igorina pusilla*

Definition: The biostratigraphic interval is defined by *Igorina pusilla* between the LO of *Morozovella angulata* and the LO of *Igorina albeari*.

Estimated age: early Late Paleocene (Danian).

Occurrence: It attains a thickness of about 1.5 m (samples 31 to 33) (Fig. 2).

4.3.2 Subzone P3b. *Igorina albeari*

Definition: It ranges from Globanomalina pseudomenardii's LO to Igorina albeari's LO.

Estimated age: middle Paleocene (Selandian).

Occurrence: At the Gebel Kilabiya section, it reaches a thickness of roughly 3 m (samples 34–39) (Fig. 2).

5 Results

5.1 Foraminiferal parameters

One of the most effective methods for determining paleobathymetry is the benthic foraminifera test. Using foraminiferal indicators such as (TFN), (BFN), (PFN), Index of Oceanity (P%), and Diversity, many researchers have utilized the depositional depths of individual species and faunal assemblages. (Fig. 3). The micropaleontological examination of the benthic foraminiferal content reach 52 species belonging to 33 genera.

5.1.1 Total foraminiferal number (TFN)

The total foraminifera number, which is roughly 300 in rich samples and 50 in poor ones, is used to represent the TFN [36]. Generally speaking, increases in the overall number of foraminifera are the outcome of the dominant favorable conditions for the foraminiferal community. As a result, TFN values represent the condition of the water depth, with an enhance in TFN typically denoting a deeper water depth. However, it isn't an independent parameter but it should be coupled with other parameters (Fig. 3).

Within the P1c subzones, the TFN values increased from 264 to 292 individuals. All samples except sample 19 have significant TFN levels in the P2 zone, where it reached a minimum of 82 individuals. In samples 27–29 (P2 Subzone), the **TFN** values oscillated from 323 to 255 individuals (Fig. 3).

5.1.1.1 Benthic foraminiferal number (BFN) According to Kaiho and Hasegawa [37] and [38], the BFN is a suitable proxy for estimating oxygen levels and the flow of organic matter in the past. The BFN typically declines in oxygen-depleted sediments [39] and [40], as organic matter transport to the bottom increases, however, a higher BFN is recognized in the work of [41]; [38], and [42]. As a result, both the oxygen concentration and the flux of organic matter affect the BFN. Mendes et al. [43] documented an inverse relationship between the BFN and water depth (Fig. 3).

In P1c Subzones the **BFN** values increase upward from 71 to 115 individuals. The **BFN** values in the P2 Zone are high in samples 8–26, except sample 9, where it reaches a minimum of 34 individuals. In samples, 27–29, the **BFN** values oscillate again from 263 to 228 individuals (Fig. 3).

5.1.2 The Planktic foraminiferal number (PFN)

The **PFN** ranges from 1 to 312 individuals in the studied section (Fig. 3). In P1c Subzones, the **PFN** values decreased from 193 to 177 individuals. The **PFN** values in the P2 Zone are high in samples 16–28, except sample 22 reaches a minimum of 1 individual. In samples 38–39 (P3b Subzone), the **PFN** values oscillate again from 40 to 27 individuals (Fig. 3).

5.1.3 The index of Oceanity (P %)

A low percentage of planktic foraminifera 8–25% dominates the middle shelf (50–100 m), which has increased species diversity. The inner shelf (10–50 m) is distinguished by an uncommon planktic percentage (8%) with low species diversity. On the other hand, the middle slope (400–800 m) is characterized to have a P% of 90%; whereas the outer shelf environment (100–200 m) has a high P% of 70% [44].

In the present study, the **P%** in samples 7 and 8 (P1c Subzones) is ranging between 61 and 73%. In samples 16–22 (P2 Zone), the **P%** increases upwards from 47 to 87% and then decreases again from 38 to 1% in samples 30–32 (P3a Zone). In samples, 35–37 (P3b Subzone), the **P%** is low (9–13%) and decreases from 13 to 9% in samples 38–39 (Fig. 3).

5.1.4 The diversity indices

The number of benthic species is correlated with species richness (S) using diversity indexes. Some diversity indices, including Shannon–Weaver, Fisher's alpha, and species richness, were used in the current study to quantify biodiversity. According to several studies [45] and [46], species diversity often rises with increasing paleodepth.

The **species richness** in samples 7 and 8 (P1c Subzone) begins to increase by 18–28 species/sample. During the Danian period, samples 7–26 show an increase in the species richness of benthic foraminifera from 15 to 41 species/sample, where in P3a Subzones (samples 31–33), it reaches 46 species/sample except sample 32 reaches a minimum of 27 species/sample (Fig. 3).

5.1.5 Calcareous/Arenaceous ratio (C/A)

According to Polski [47] and [48], the arenaceous benthic foraminifera could live in a variety of environments, from very shallow marine to abyssal. The predominance of calcareous foraminifera points to sedimentation that occurred well above the carbonate compensation depth (CCD), in a zone

with high calcium carbonate concentrations, good oxygenation, and/or normal salinity [49]. Figure 3 shows the C/A for the Gebel Kilabiya section.

In the succession under investigation, 52 species of benthic foraminifera belonging to 33 genera have been identified. Calcareous species, which significantly dominate the fauna and exhibit deposition much above the CCD, are present in more than 63% of all samples [45] and [46].

5.1.6 Epifaunal/infaunal ratio

Changes in the ratio of these morphotypes could be a sign of the modifications in the flux of organic carbon and/or Paleo-oxygenation [50]. Numerous studies such as [51] and [38] have shown a correlation between the various microhabitats in which benthic foraminifera are found and the percentage of the epifauna. Bernhard [52] mentioned that epifaunal species frequently suggest high oxygen levels and/or low nutrition concentrations. Epifaunal morphotypes living at the sediment–water interface usually have test of a low surface area to volume ratio (plano-convex trochospiral, trochospiral, biconvex trochospiral, and rounded trochospiral shapes). These morphotypes are only can be lived within well-oxygenated bottom water. In general, epifaunal taxa (Table 2) are less resilient to low oxygen concentrations and high food fluxes.

The test morphology of infaunal species in sediments usually has a high surface area to volume ratio (tapered, cylindrical, flattened ovoid, spherical, rounded planispiral, and uni, bi-, triserial forms). Infaunal species can exist in situations with low oxygen levels. The abundance of infaunal forms is favored by low oxygen levels and/or high fluxes of organic matter (e.g., [52] and [41]).

In the present study, **Epifaunal/Infaunal** ratios range from 8.33 to 93.75 indicating vary from oligotrophic to eutrophic-mesotrophic conditions (Fig. 3). Tables 2 and 3 show the epifaunal and infaunal benthic foraminiferal taxa in the Kilabiya section.

5.1.7 Depth-controlled benthic foraminiferal assemblages

Tests for benthic foraminifera are frequently employed as markers of paleobathymetry because some depth-related parameters regulate their depth distribution in the oceans (e.g., [45] and [53]). We were thus able to deduce the paleobathymetry of the Paleocene succession at Kalibiya through the examination of modern and fossilized assemblages, the prevalence and size of species associated with depth, and the upper limits of these species (e.g., [53, 54] and [55]). The benthic foraminifera can be divided into two groups [51], Midway-fauna (**MF**) and Velasco-fauna (**VF**) (Table 4).

5.1.7.1 The Midway-fauna (MF) (continental shelf) The benthic assemblages found in the lower Paleocene Midway Formation (Texas), which were initially investigated by [57] and [58], served as the model for the Midway fauna (MF) of [56]. Their species occur in neritic marl/shale deposits [59]; and [60]. This assemblage consists of calcareous and arenaceous benthic foraminifera, abundant to common planktic. Benthic foraminiferal species diversity is high from the middle to the outer shelf. The Velasco-fauna (VF) (bathyal and abyssal depths)

The lower Paleocene Velasco-Shale Formation (Mexico) is the source of the Velasco-fauna (VF) [55]. The initial descriptions of its foraminiferal contents were from [61, 62] and. According to Saint-Marc and Berggren

Table 2 Epifaunal benthic foraminiferal taxa in the Kilabiya section

EPIFAUNAL morphotype		
Calcareous test		
Biconvex Trochospiral	Trochospiral Plano-convex	Palmate
Anomalinoides acuta	*Alabamina midwayensis*	*Frondicularia archiaciana*
Anomalinoides praeacutus	*Angulogavelinella avnimelechi*	*Frondicularia frankei*
Anomalinoides affinis	*Cancris auricular*	*Neoflabellina semireticulata*
Cibicidoides alleni	*Cibicidoides succedens*	**Rounded Trochospiral**
Cibicidoides pseudoperlucides	*Gyroidinoides girardanus*	*Valvulineria scrobiculata*
Cibicidoides pseudoacutus	*Valvalabamina depressa*	
Lenticulina spp.		
Osangularia plummerae		
Arenaceous test		
	Coiled flattened	
	Ammodiscus cretaceous	

Table 3 Infaunal benthic foraminiferal taxa in the Kilabiya section

INFAUNAL morphotype		
Calcareous test		
Elongate	Flattened tapered	Spherical/globose
Bulimina farafraensis	*Loxostomoides applinae*	*Lagena apiculate*
Bulimina midwayensis	*Marginulina carri*	*Lagena hispida*
Bulimina quadrata	*Marginulinopsis tuberculate*	
Bulimina reussi	*Vaginulina cretacea*	
Laevidentalina colei	**Tubular or branching**	
Stilostomella paleocenica	*Ramulina navarroana*	
Orthokarestenia oveyi		
Orthokarestenia parva		
Arenaceous test		
Elongate multilocular		
Gaudryina aissana	*Clavulinoides asper*	*Spiroplectinella dentata*
Gaudryina cf. *ellisorae*	*Clavulinoides trilateral*	*Spiroplectinella esnaensis*
Gaudryina laevigata	*Dorothia bulletta*	*Spiroplectinella henryi*
Gaudryina nekhlensis	*Dorothia oxycona*	*Spiroplectinella knebeli*
Gaudryina pyramidata	*Textularia farafraensis*	*Spiroplectinella spectabilis*
Gaudryina soldadoensis	*Textularia schwageri*	*Vulvulina colei*
Gaudryina rugosa	*Tritaxia midwayensis*	
Marssonella indentata	*Tritaxia trilateral*	

Table 4 Midway-fauna Type (**MF**) and Velasco-fauna Type in the Kilabiya section

Midway-fauna type (MF)	Velasco-fauna (VF)
Anomalinoides acuta	*Angulogavelinella avnimelechi*
Anomalinoides midwayensis	*Laevidentalina colei*
Bulimina quadrata	*Orthokarestenia oveyi*
Cibicidoides alleni	*Ramulina navarroana*
Cibicidoides pseudoperlucides	*Stilostomella paleocenica*
Cibicidoides succedens	*Neoflabellina semireticulata*
Lagena apiculate	*Spiroplectinella henryi*
Lagena hispida	*Spiroplectinella dentata*
Lenticulina spp.	*Tritaxia midwayensis*
Loxostomoides applinae	
Marginulinopsis tuberculate	
Spiroplectinella esnaensis	

(1988) [63], the VF is frequently identified in bathyal and abyssal deposits [56] as well as in "outer neritic to bathyal" deposits. In the studied section, the **VF** assemblages were recorded by [60] and [64] as Midway-fauna.

5.1.8 Benthic foraminiferal biofacies

The quantitative examination of assemblages of benthic foraminifera aids in the interpretation of depositional environments and variations in sea level. The distribution charts of the region under study show the dominant benthic foraminiferal species in each frequency and cluster, with relative abundances of more than 3 and 5% (Fig. 9).

Four major clusters (I, II, III, and IV) were defined as a result of the R-Mode cluster analysis of the benthonic foraminiferal in the area under study. The dominant depth-significant taxon of each component biofacies is the basis of the biofacie's designations.

In the Paleocene interval, the authors used 40 species belonging to 33 genera have been recognized. Four benthic foraminiferal biofacies in the present study are described from shallower to deeper biofacies (Fig. 10) as follows:

Cluster I: it is primarily comprised of calcareous and arenaceous benthic foraminifera; planktic foraminifera are rare, and there is a significant abundance of low-diversity benthic species. Commonly occurring, calcareous benthic foraminifera are characterized by dominated abundance and little diversity.

This assemblage is generally containing *Gaudryina ellisorae*, *Spiroplectinella dentate, S. henryi, Anomalinoides affinis, Alabamina midwayensis, Cibicidoides alleni,* and

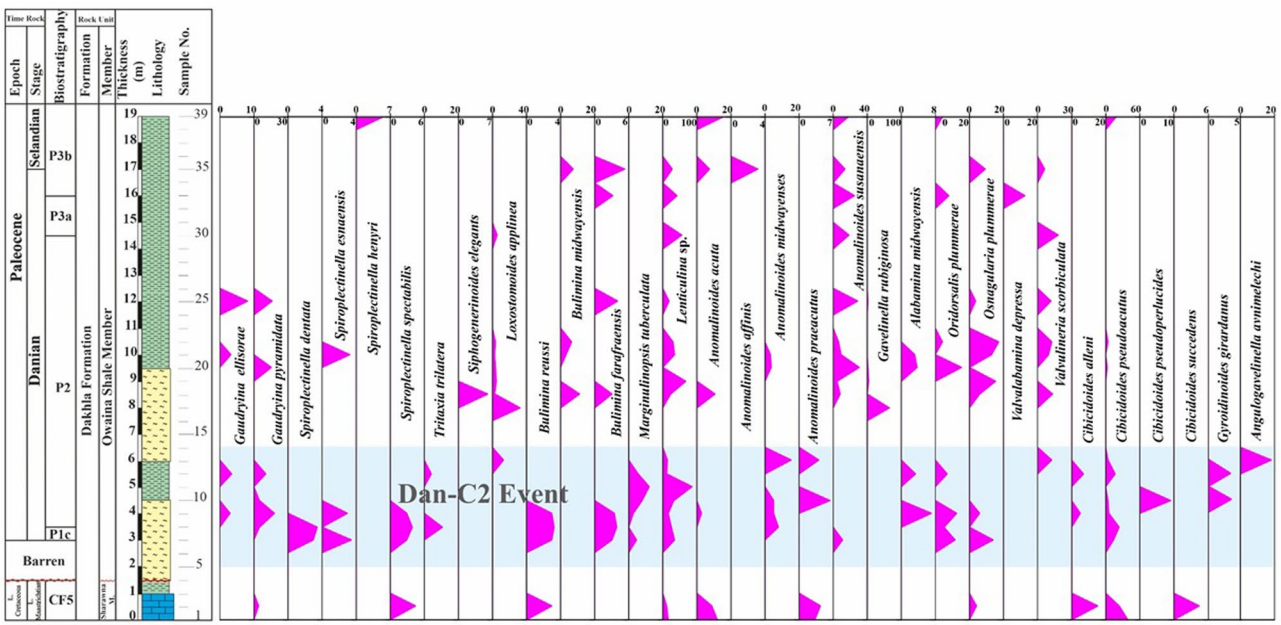

Fig. 9 Benthic foraminifera distribution with Dan-C2 event in Gebel Kilabiya section

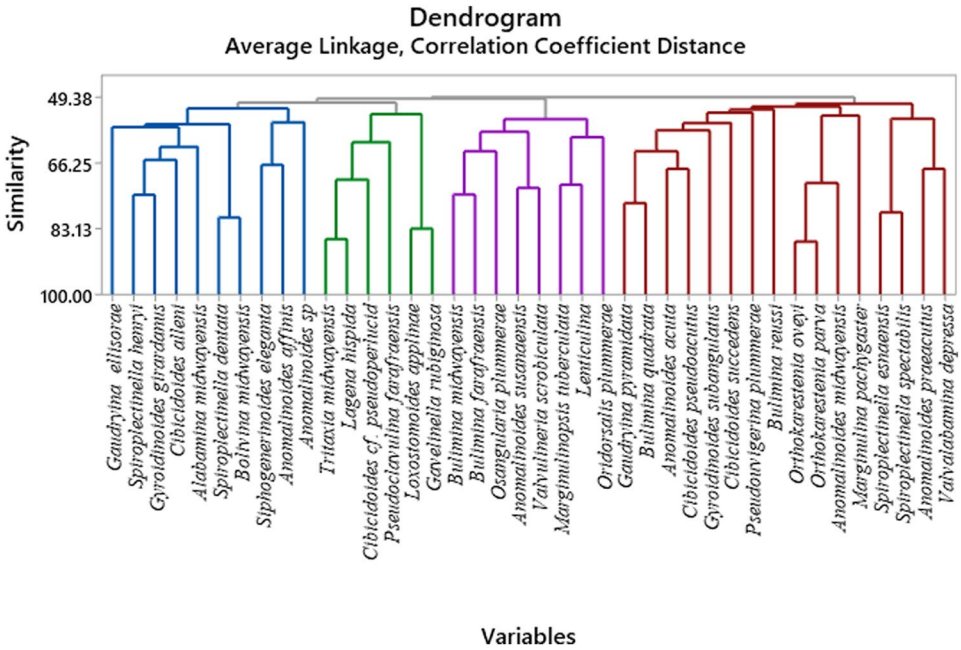

Fig. 10 Stratigraphy, benthic foraminifera $\delta^{13}C$, and $\delta^{18}O$ measurements on the Kilabiya section: (1) $\delta^{13}C$ chemostratigraphy reveals negative carbon isotope excursions at the determined LDE1 onset (62.2 Ma) in Qreiya 3 section. Since Bornemann et al. (2009) highlighted how temperature is not the primary determinant of $\delta^{18}O$ on the comparatively shallow shelf, no $\delta^{18}O$ data are presented for the Qreiya 3 area

Gyroidinoides girardanus indicating outer neritic to bathyal environments (~ 150–600 m deep).

Cluster II: is a diverse and heterogeneous assemblage with mixed infaunal and epifaunal morphogroups representative of the Midway-type fauna [56]. Among the taxa are *Gaudryina pyramidata, Spiroplectinella esnaensis, S. spectabilis, Orthokarestenia oveyi, O. parva, Bulimina quadrata, B. reussi, Marginulina carri, Anomalinoides acuta, A. midwayensis, A. praeacutus, Valvalabamina depressa, Cibicidoides pseudoacutus, C. succedens* and *Gyroidinoides girardanus.* The composition of the assemblage and the diversity of benthic foraminifera indicate an outer neritic to bathyal environment (100–600 m).

Cluster III: mostly consists of epifaunal and infaunal species that prevail among calcareous and arenaceous benthic foraminifera with a high diversity and P/B%. The assemblage is dominated by *Tritaxia midwayensis, Lagena hispida, Loxostomoides applinae, Gavelinella rubiginosa,*

and *Cibicidoides pseudoperlucides.* The diversity of benthic foraminifera and the composition of the assemblage point to an outer neritic to bathyal environment (< 100 m).

Cluster IV: mainly consists of calcareous and arenaceous benthic foraminifera, the majority of species are infaunal and epifaunal with a high diversity and P/B%. The assemblage is dominated by *Bulimina midwayensis, B. farafraensis, Marginulinopsis tuberculate, Lenticulina* spp.*, Osangularia plummerae* and *Valvulineria scrobiculata*. The diversity of benthic foraminifera and the composition of the assemblage point to an outer neritic environment (100–200 m).

5.2 Carbon and oxygen isotope anomalies

In addition to the large reduction in $CaCO_3$, the LDE beds are linked to negative shifts in $\delta^{13}C$ and $\delta^{18}O$ in benthic foraminifera. Benthic foraminifera tests were found to have a negative CIE of up to 2‰ by [1] at several Egyptian shelf sections. As a result, the negative CIE appears a characteristic of the LDE and the Dan-C2 event (Fig. 8).

Considering the structure and comparison of variants of δ13C among the various sites, our results indicate that the LDE critical interval is correlative with the LDE interval of the Qreiya 3 section of [15] and is, therefore, the sedimentary expression of the LDE event in this part of the Eastern Tethyan Ocean (Fig. 8).

6 Discussion

6.1 Benthic foraminiferal assemblages

Throughout the examined segment, the preservation of benthic and planktic foraminifera is generally satisfactory (Figs. 4–7). The assemblages are dominated by calcareous (average of 92%) and epifaunal species (average of 70%) (Table 2, 3). *Bulimina* spp., Trochospiral *Cibicidoides* spp., and *Anomalinoides* spp., with average abundances of 2.1, 2.8, and 3.2%, respectively, are the most prevalent epifaunal taxa. The most prevalent infaunal species is *Spiroplectinella spectabilis* (average of 1.2%), which comprises the most common agglutinated taxa, together with *Clavulinoides asper* and *Cl. trilateral*.

The diversity and heterogeneity indices, which define the pre-event phase, show strong swings on a modest trend drop (Fig. 3). A rise in the percentage of agglutinated taxa is connected with a progressive decrease in the % $CaCO_3$ content. Over this time, the absolute abundance of benthic foraminifera drops, in contrast to uniserial lagenids and polymorphinids. The maximum absolute abundance of benthic foraminifera and the lowest diversity values (samples 7–8) are both found in the Dan-C2 interval.

The increase in the relative abundance of agglutinated species (up to 22% of the assemblages) in the middle of Dan-C2 is unrelated to the decrease in $CaCO_3$ content. Throughout the event, infaunal morphogroups such as unilocular species, polymorphinids, and unserial lagenids show the lowest relative abundance.

Heterogeneity and diversity increase steadily above Dan-C2 (Fig. 3) in the upper section of the analyzed interval. Several infaunal taxa (buliminids, uniserial lagenids, polymorphinids, and unilocular taxa) have slightly higher percentages than the Dan-C2, in contrast to agglutinated species. Over time, the abundance of epifaunal taxa loses above Dan-C2.

6.2 Planktic foraminiferal assemblages

Planktic foraminiferal faunas consist of about 86% of the overall assemblage and are dominated by eight genera and twenty species (Fig. 11). The stratigraphic description of them based on their abundance maxima as follows:

Before the LDE, *praemurica uncinata* was relatively common (26%) but nearly disappeared at the base of the LDE. Similar trends are shown with *P. inconstans*, a fewer common species. *Morozovella acuta* exhibits a large breakdown around the first LDE horizon and rapidly decreases to 10% from sample 30 below the LDE (Fig. 11).

While *Morozovella angulata* steadily increases from 2 to 3% across the research interval at the first LDE horizon, *Morozovella aequa* only sometimes appears but is present over the whole study area. The LED peaks reach a maximum of 46% of the lowest LDE peak just before and during the event.

The marker species for Subzone P3b is *Igorina albeari* and is present for the whole studying interval, suggesting that the P3b's base lies much below the LDE in the Kilabiya section. When the LDE commences, its abundance increases from 1 to 5% at the beginning. Additionally, *Subbotina velascoensis* exhibits a modest increase up to 90% before the LDE, a decline down to 10–15% during the event, and a recovery up to ~ 20% afterward (Fig. 3).

6.3 Paleoenvironmental interpretation

6.3.1 P1c Subzone

The shallow water conditions (middle neritic depth 30–100 m) are showed by the decrease in the P/B ratio from 0.7 to 0.3, associated with the drop in planktic percentage from 45 to 24% and species diversity from 19 to 5 species.

The benthic assemblages (*Spiroplectinella, Dorothia, Textularia*, *Tritaxia*, *Gaudryina, Cibicidoides, Lenticulina*, *Anomalinoides*, *Gyroidinoides*, *Marginulinopsis*, *Valvulineria*, and *Lagena*) confirm this paleobathymetric

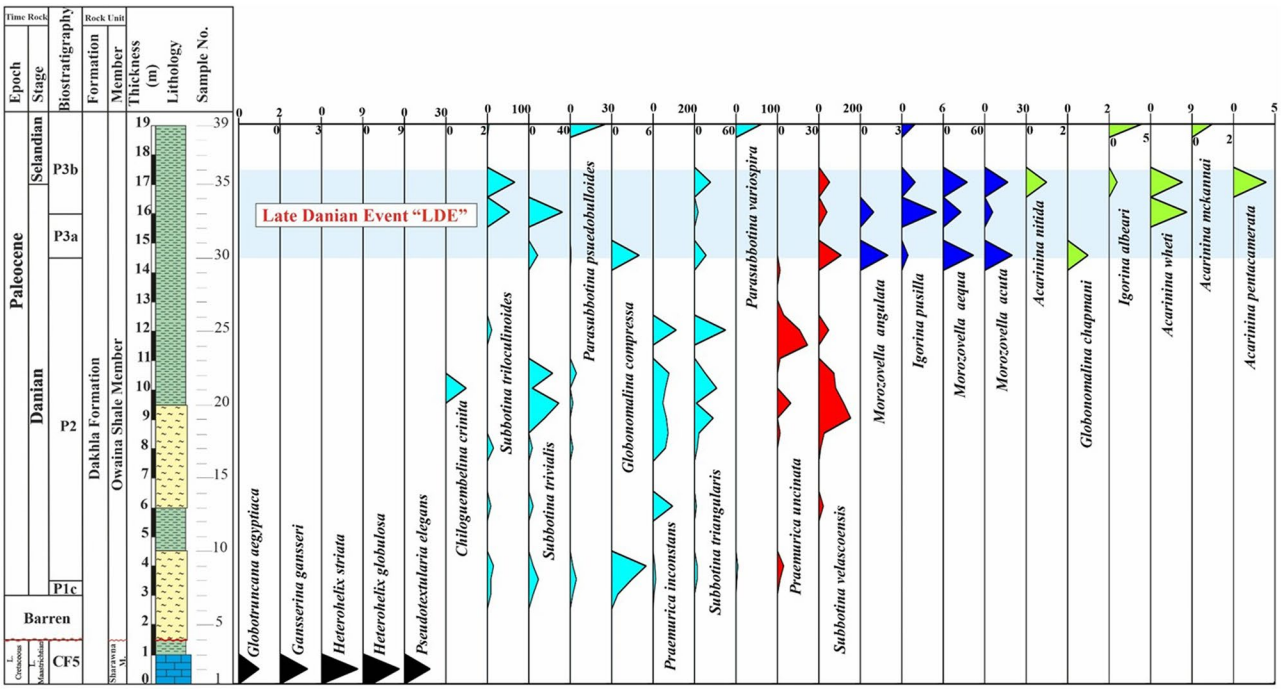

Fig. 11 Planktic foraminifera distribution with Late Danian Event (LAD) in the studied section

interpretation, which is similar to the inner shelf (0–100 m depth) modern assemblage of [65]. Meanwhile, at the upper part of this Subzone (sample 8), the recorded benthonic foraminifera are exactly the same as the base, with the exception of *Neoflabellina*, *Stilostomella*, *Frondicularia*, *Pseudonodosaria*, and *Vulvulina* which means that the deep water morphogroups (tubular and globular occurring in low amounts in the upper part of the Dakhla Formation) suggest a relatively deeper environment than the lower part as suggested by [65].

The lowest part of the P1c Subzone is characterized by a notable concentration of calcareous agglutinated foraminifera. Granular calcite and hyaline tests are abundant and are linked to the warm water basin when a suitable amount of calcium carbonate is dissolved in the water [66]. The P1c Subzone in the section under investigation coincides with the onset of the warming event, according to Boersma et al. [67]. Planktic foraminifera with warm water morphotypes were prevalent in this area, as indicated by the presence of morozovellids and acarininids.

Variations in the percentages of arenaceous and calcareous agglutinated foraminifera identify the upper part. These characters indicate an outer neritic environment with very small oscillation at its upper part represented by the inner neritic environment. The uppermost part of this Subzone contains only arenaceous agglutinated foraminifera of simple wall arenaceous foraminifera. *Ammobaculites* and *Haplophragmoides* predominate in this area, indicating a strong organic flux and extremely dysaerobic conditions caused by freshwater discharge. This area is classified as oxygen-depleted environment (shallow to deep littoral) [60, 68–70] and [71].

6.3.2 P2 Zone

Nearly all of the foraminiferal assemblages in the Kilabiya section of the lower P2 Zone (early Danian) are agglutinated species, which are thought to be associated with brackish or stagnant conditions (samples 8–15) [72] and [73]. The comparatively high diversity displayed by agglutinated foraminiferal assemblages (from 16 to 28) also rules out brackish conditions. The increasing assemblages of agglutinated foraminifera indicate that lower pH and dysaerobic bottom conditions occurred in the depositional region. These conditions would have prevented calcareous assemblages, as they were likely less resilient to low pH and dysoxia than agglutinated faunas [73].

A notable concentration of calcareous agglutinated foraminifera in the lowest portion of the P1c Subzone is what sets it apart. The warm water basin is connected with an abundance of granular calcite and hyaline tests that may be visible when a sufficient amount of calcium carbonate is dissolved in the water (Fig. 7) [66] and [67], the P1c Subzone in the investigated section is where the warming event began. Here, warm water morphotypes of planktic

foraminifera were abundant, where the existence of morozovellids and acarininids suggests high paleotemperatures.

The predominance of calcareous benthic foraminiferal taxa that are well-preserved suggests deposition that occurred considerably above the CCD. Benthic foraminiferal morphogroups are indicative of meso-oligotrophic conditions, meaning that there is sufficient organic material transfer to the bottom to support epifaunal and infaunal foraminifera, according to Jorissen et al. [38]. Since oxygenation was not a limiting factor and no extremely numerous oxygen-tolerant species present, we can conclude that there is no organic enrichment or lamination in the sediments even in the samples of lowest diversity.

Hull and Norris [74] claim that environmental stress at the seafloor is shown by differences in the assemblage's heterogeneity and diversity before and during Dan-C2., which may be caused by primary productivity's instability and variability following the K/Pg impact event (Fig. 3). The increasing of agglutinated tests in Dan-C2 was mostly caused by an increase of *Spiroplectinella spectabilis* (infaunal). Since this species uses Ca Co_3 to agglutinate [75], carbonate dissolution was not the source of its growth.

6.4 Dan-C2 event

Samples 1–9 in the Kilabiya section, which includes the upper, maybe the sedimentary expression of a second brief hyperthermal event. The earliest peaks, in particular, match quite well.

The low diversity of the subsequent survival interval is dominated by agglutinated foraminifera (samples 7 and 8). Opportunistic taxa become more abundant, and the relative quantity of arriving taxa like *Cibicidoides*, *Bulimina*, and *Gyroidinoides* steadily rises (Fig. 9). Furthermore, in the Dan-C2 event, the proportion of agglutinated foraminifera increases and the planktic foraminifera values are significantly greater. These indicators point to significant alterations in the chemistry of the ocean as well as an acceleration of dissolution.

The Dan-C2 event is characterized by greater levels of benthic foraminiferal density and infaunal morphogroups, which point to an increased food supply to the bottom. This could mean enhanced eutrophication and/or a recovery of the food web. Regarded as taxa associated with recolonization and enhanced organic flow [76], *Reophax* and *Spiroplectinella* show increased abundances during the Dan-C2 event. Typically, these benthic taxa are referred to as opportunists. The elongated subcylindrical taxa, *Marssonella* and *Dorothia*, are abundant during the Dan-C2 event (Table 5). These taxa evolved to flourish in more eutrophic environments with higher levels of organic flow and typically predominate in low-oxygen environments.

Table 5 Parameters recorded during the Pre-event and Post-event of the Dan-C2

Parameters	Pre-event	Dan-C2	Post-event
Diversity (Fisher- α)	19.4	17.7	21.1
Heterogeneity (H(S))	3.4	3.3	3.4
Foraminiferal density	76,276	481,652	11,680
Agglutinated taxa %	8.8	14.2	11.5
Infaunal taxa %	47.1	39.8	46.3
Buliminids %	4.5	5.3	0.7
Uniserial Lagenids %	4.5	1.4	3.7
Unilocular Taxa %	1.2	0.9	1.6
Polymorphinids %	2.2	1.1	3.0

At the early Paleogene, the deep-sea floor experienced unstable environmental circumstances, as demonstrated by the examination of benthic foraminifera from the Kilabiya section. Due to the mass extinction of K/Pg, these conditions were probably affected by changes in primary producers, both calcareous and non-calcifying. The sea-surface biota, which was still recovering from the K/Pg extinction, might have been impacted by this volcanic activity [77].

6.5 The late Danian event (LDE)

Within the shales of the Dakhla Formation, the LDE beds are intercalated near to the P3a/P3b boundary in the Kilabiya area [32]. There are two different beds (1 and 2) in the LDE deposit. Bed 1 (samples 30–35) has an abundance of planktic foraminifers, laminated organic-rich soil, and dark clay. Parallel to the lamination in Bed 2 are dark grey clay lenses (sample 36).

Subbotina, a group of mesotrophic subsurface taxa, dominate the planktic foraminiferal assemblages in the Kilabiya region during the study interval, while *Morozovella* species, a group of warm, oligotrophic surface waters, predominate the Egyptian shelf (Fig. 11).

During the study interval, the proportional abundances of Morozovella increased. and more especially, *M. angulata*. The assemblages of planktic foraminifera exhibit a constant change over time. There has been evidence of this long-term transition, which supports the idea that *M. angulata* evolved from Praemurica uncinata [78]. Additionally, the *Praemurica* disappearance near the base of the LDE is mostly synchronous in the Kilabiya region, and it is accompanied by a long-term, steady increase in *Morozovella* abundance. In particular, in the Kilabiya region, both relative and absolute abundances of *Morozovella* within the P3a-P3b Subzones of LDE have been seen, indicating surface-water warming (Fig. 11).

The Kilabiya section results demonstrate the faunal changes, including the extinction of the *Praemurica* before

the LDE at sample 32. The extinction of this taxon is demonstrated by the deep-sea records, the Wombat Plateau (Indian Ocean) [79], data from Qreiya 3 section (Egypt), Tunisia, and Jordan [80] and [81].

Our findings imply that the LDE-related environmental changes exceeded a particular threshold, leading to a persistent change in the biota of the ocean's surface. Photo symbiosis was first developed in planktic foraminifera [82].

6.5.1 Biostratigraphic implications

The LDE has typically been located at or slightly above the P3a/P3b Subzone boundary, based on planktic foraminifera biostratigraphy [5]; [83] and [14]. This boundary was determined by the first appearance of *Igorina albeari* [35] and [32].

Even though Soldan et al. [84] identified that *I. albeari* maybe having a close relationship species, we carefully follow the taxonomic description of Olsson et al. (1999) [31]. It is therefore suggested that the P3a/P3b boundary is much below the LDE. Based on its early occurrence at the Kilabiya section, we speculatively suggest perhaps this species descended from *Igorina pusilla* in the Pacific and appeared later in other ocean basins. Furthermore, individuals with minor morphological changes from *G. pseudomenardii* were discovered and given the name *G. pseudomenardii* since they prevent the definitive identification of the species.

In earlier investigations, it was found that the LDE and the LO *Morozovella angulata* are stratigraphically adjacent in the planktic foraminiferal Subzones P3a and P3b. Since the P3a boundary in this zonation is located around 1 Myr of the upper Danian planktic foraminifera to the lowest Selandian age needs to be revised. More events must be added to resolution of the extended P3a Subzone. As a result, the LO of *Praemurica uncinata* and the FO of *Morozovella angulata* were found.

The disappearance of the planktic foraminifer genus *Praemurica* in the studied region at the beginning of, or just inside of, the LDE provides evidence that the extinction is simultaneous on a nearly global scale. Over time, the relative abundance of morozovellids increases as praemuricids spread.

The LDE separates the observed temperature increase that started before the collapse of *Praemurica* by an increase in thermophile species (morozovellids) providing more evidence for the LDE warming. The North Atlantic Igneous Province's volcanic activity is responsible for the long-term temperature and faunal changes that have been seen [85]. The event's extreme orbital configuration or additional CO2 from other sources may have caused the momentary warming and faunal response at the LDE. Lastly, we find that the LO of Praemurica has a more stable extension in the studied Kilabiya area of the upper Danian-lower Selandian.

6.5.2 Paleoenvironmental implications

During P1c Subzone the shallow water conditions (middle neritic depth 30–100 m) are indicated by the decrease in the P/B ratio from 0.7 to 0.3, associated with the drop in planktic percentage from 45 to 24% and species diversity from 19 to 5.

The depositional basin gradually deepens in the P3a Subzone of the Kilabiya section, starting at the top of the Dakhla Formation and extending to P3b. Furthermore, the higher infaunal morphogroup percentages in the P3a Subzone point to an increase in the flow of nutrients to the sea floor. Therefore, instead of the Selandian seafloor waters having low oxygen levels, we infer moderate to high production.

7 Summary and conclusion

7.1 Dan-C2 event

By comparison to typical Paleogene hyperthermal episodes (such as PETM, ETM2, and ETM3 [19], benthic foraminifera's mild response to Dan-C2 is shown by our data to be markedly different. Strong evidence exists to suggest that the increased mineralization of organic matter brought on by bottom-water warming reduced the amount of food available to the benthos (see, for example, [86]; [87] and [88]). This record and our findings indicate that only minority occurred in the benthic taxa during the event, with agglutinated forms showing just a slight increase in relative abundance. The authors hypothesized that increases in eutrophication and/or the restoration of the food chain were the causes of the observed increase in the benthic foraminifera through the Dan-C2.

Benthic foraminiferal assemblages reveal that trophic conditions steadily improved towards the end of the study interval, first under more agitated conditions (dominance of cluster II), then the food supply stabilized.

7.2 LDE event

When it comes to their elimination at the lowest LDE peak, *Praemurica uncinata* and P. inconstans exhibit parallel patterns in abundance (Fig. 11). This indicates that, in comparison to *Morozovella* species occupying an equivalent ecological niche, this group was less competitive. It is strongly influenced by LDE-associated environmental changes, such as temperature shifts and disruptions to the carbon cycle.

Praemurica demise at or near this stratigraphic level in shelf successions from the Tethys Ocean [81]. In the northeastern Atlantic, the latest Danian shows a similar faunal shift [89]. The ecological adaptation of *M. angulata* to LDE and post-LDE surface conditions appears to be superior. The

LDE at the Kilabiya section suggests a permanent increase in *M. angulata* (Fig. 11). Surface water conditions above the LDE favored *Morozovell'*s predominance. Most *Morozovella* species show a sustained increase in relative abundance and seem better suited to surface water that is warm, stratified, and oligotrophic.

Parasubbotina pseudobulloides profited from the changes in oceanography caused by the LDE (Fig. 11). *Parasubbotina pseudobulloides* was a very productive species during the LDE. A full ecological explanation is not feasible because in the late Danian there is relative rarity of related *Subbotina* spp.

This instance of extinction is synchronized on a practically global scale, as evidenced by the loss of the planktic *Praemurica* in the examined area within the LDE. The relative abundance of morozovellids rises with the proliferation of praemuricids throughout time. The extent of *Praemurica* and the observed temperature rise that started before the LDE are separated by the LDE. The North Atlantic Igneous Province's volcanic activity is related to the long-term shift in flora and temperature that has been recorded.

Paleotemperature interpretation requires fluctuation in the abundance of fraction (> 63 µm) of planktic foraminifera. In this regard, [90] provided evidence that the low-latitude group comprises warm morphogroups such as, *Igorina, Morozovella, Praemurica* and *Acarinina*. The high latitude includes the cold morphogroups *Parasubbotina, Eoglobigerina*, *Subbotina,* and *Globanomalina* (Fig. 11). The P1c Subzone was the starting point of the warming event, which extended to the P2 Zone. The low-latitude, which includes the warm morphogroups *Igorina, Acarinina*, *Morozovella,* and *Praemurica*, outnumbers the high-latitude, which includes the cold morphogroups *Subbotina, Parasubbotina, Eoglobigerina,* and *Globanomalina*, during the warming trend that occurs during the (Subzone P3a and P3b).

Acknowledgements We are grateful to the soul of Prof. Dr. Molina from Universidad de Zaragoza, Spain, for the stable isotope measurements and to Prof. Dr. Ahmed El-Sabbagh and Prof. Dr. Ahmed S. Mansour from Alexandria University for their constructive reviews of an earlier draft of the manuscript and their constructive comments and advice. We greatly appreciate the organizations that funded this research.

Author's contribution All authors contributed to the study conception and design. Material preparation, data collection, and analysis were performed by [Dr. Heba Ismail], and [Dr. Saida Taha]. The first draft of the manuscript was written by [Prof Dr. Orabi H. Orabi] and all authors commented on previous versions of the manuscript. All authors read and approved the final manuscript.

Funding The authors did not receive support from any organization for the submitted work.

Data availability The data are available as: to obtain clean fossils, 50 g of each sample was soaked in Hydrogen Peroxide solution (10% H2O2), washed over a 63-mesh sieve, and then dried and sieved into fractions greater than 250, 125, and 63 mesh. The fraction 63 µm was chosen because it is thought to be the most suitable for studying the benthic and planktic community. Under a binocular microscope at a magnification of 50, planktic foraminifera tests were recognized. At Alexandria University, scanning electron microscopy (JEOL JSM-5500 LV) is used to take pictures of the most significant planktic foraminifera. The relative frequency data of benthonic foraminifera in the section is subjected to cluster analysis. The statistical analysis is performed, using the "Minitab", the species with a relative frequency of 5% are excluded.

Declaration

Conflict of interest All authors declared that there is no conflict of interest.

References

1. Bornemann A, Schulte P, Sprong J, Steurbaut E, Youssef M, Speijer RP (2009) Latest Danian carbon isotope anomaly and associated environmental change in the southern Tethys (Nile basin, Egypt). J Geol Soc 166:1135–1142. https://doi.org/10.1144/0016-76492008-104
2. Westerhold T, Röhl U, Wilkens RH, Gingerich PD, Clyde WC, Wing SL, Bowen GJ, Kraus MJ (2018) Synchronizing early Eocene deep-sea and continental records—cyclostratigraphic age models for the Bighorn Basin Coring Project drill cores. Clim. 14:393–319. https://doi.org/10.5194/cp-14-303-2018
3. Westerhold T, Marwan N, Drury AJ, Liebrand D, Agnini C, Anagnostou E, Barnet JSK, Bohaty SM, De Vleeschouwer D, Florindo F, Frederichs T, Hodell DA, Holbourn AE, Kroon D, Lauretano V, Littler K, Lourens LJ, Lyle M, Pälike H, Röhl U, Tian J, Wilkens RH, Wilson PA, Zachos JC (2020) An astronomically dated record of Earth's climate and its predictability over the last 66 million years. Science 369:1383–1387. https://doi.org/10.1126/science.aba6853
4. Coccioni R, Frontalini F, Bancalà G, Fornaciari E, Jovane L, Sprovieri M (2010) The Dan-C2 hyperthermal event at Gubbio (Italy): global implications, environmental effects, and cause(s). Earth Planet Sci Lett 297(1–2):298–305. https://doi.org/10.1016/j.epsl.2010.06.031
5. Bralower TJ, Cosmidis J, Heaney PJ, Kump LR, Morgan JV, Harper DT, Lyons SL, Freeman KH, Grice K, Wendler JE, Zachos JC, Artemieva N, Si AC, Gulick SPS, House CH, Jones HL, Lowery CM, Nims C, Schaefer B, Thomas E, Vajda V (2020) Origin of a global carbonate layer deposited in the aftermath of the Cretaceous-Paleogene boundary impact. Earth Planet Sci Lett. 548:115476. https://doi.org/10.1016/j.epsl.2020.116476

6. Petrizzo MR (2005) An early late Paleocene event on Shatsky Rise, northwest Pacific Ocean (ODP Leg 198), Evidence from planktonic foraminiferal assemblages. Proc ODP Sci Results 198:1–29. https://doi.org/10.2973/odp.proc.sr.198.102.2005
7. Stap L, Sluijs A, Thomas E, Lourens L (2009) Patterns and magnitude of deep-sea carbonate dissolution during Eocene Thermal Maximum 2 and H2, Walvis Ridge, southeastern Atlantic Ocean. Paleoceanography 24:PA1211. https://doi.org/10.1029/2008PA001655
8. Westerhold T, Röhl U, Donner B, McCarren HK, Zachos JC (2011) A complete high-resolution Paleocene benthic stable isotope record for the Central Pacific (ODP site 1209). Paleoceanography 26:PA2216. https://doi.org/10.1029/2010PA002092
9. Jehle S, Bornemann A, Lägel AF, Deprez A, Speijer RP (2019) Paleoceanographic changes across the Latest Danian Event in the South Atlantic Ocean and planktic foraminiferal response. Palaeogeogr Palaeoclimatol Palaeoecol 525:1–13
10. Deprez A, Jehle S, Bornemann A, Speijer RP (2017) Pronounced biotic and environmental change across the latest Danian warming event (LDE) at Shatsky Rise, Pacific Ocean (ODP Site 1210). Mar Micropaleontology 137:31–45
11. Barnet JSK, Littler K, Westerhold T, Kroon D, Leng MJ, Bailey I, Röhl U, Zachos JC (2019) A high-fidelity benthic stable isotope record of late Cretaceous-early Eocene climate change and carbon cycling. Paleoceanogr Paleoclimatol 34:672–691. https://doi.org/10.1029/2019PA003556
12. Westerhold T, Röhl U, Raffi I, Forniaciari E, Monechi S, Reale V, Bowles J, Evans HF (2008) Astronomical calibration of the Paleocene time. Palaeogeogr Palaeoclimatol Palaeoecol 257:377–403. https://doi.org/10.1016/j.palaeo.2007.09.016
13. Arenillas JF, Ispierto L, Millan M, Escudero D, De La Ossa NP, Dorado L, Dávalos A (2008) Metabolic syndrome and resistance to IV thrombolysis in middle cerebral artery ischemic stroke. Neurology 71(3):190–195
14. Bralower TJ, Premoli Silva I, Malone MJ (2006) Leg 198 synthesis: A remarkable 120-m.y. record of climate and oceanography from Shatsky Rise, northwest Pacific Ocean. In: Bralower, T.J., Premoli Silva, I., Malone, M.J. (Eds.), Proceedings of the Ocean Drilling Program, Scientific Results. 198: 1–47
15. Schulte P, Schwark L, Stassen P, Kouwenhoven TJ, Bornemann A, Speijer RP (2013) Black shale formation during the Latest Danian Event and the Paleocene-Eocene Thermal Maximum in Central Egypt: two of a kind? Palaeogeography, Palaeoclimatology. Palaeoecology 371:9–25. https://doi.org/10.1016/j.palaeo.2012.11.027
16. Sprong J, Kouwenhoven TJ, Bornemann A, Schulte P, Stassen P, Steurbaut E, Youssef M, Speijer RP (2012) Characterization of the Latest Danian Event by means of benthic foraminiferal assemblages along a depth transect at the southern Tethyan margin (Nile Basin, Egypt). Mar Micropaleontol 86–87:15–31
17. Deprez A, Jehle S, Bornemann A, Speijer RP (2017) Differential response at the seafloor during Palaeocene and Eocene ocean warming events at Walvis Ridge, Atlantic Ocean (ODP Site 1262). Terra Nova 29:71–76
18. Yamaguchi T, Bornemann A, Matsui H, Nishi H (2017) Latest Cretaceous/Paleocene deep-sea ostracode fauna at IODP Site U1407 (western North Atlantic) with special reference to the Cretaceous/Paleogene boundary and the Latest Danian Event. Mar Micropaleontol 135:32–44
19. Said R (1962) The geology of Egypt. Elsevier Publication Co., Amsterdam New York, p 377
20. Said R (1990) The geology of Egypt. Balkema, Rotterdam, p 721
21. Guiraud R, Bosworth W, Thierry J, Delplanque A (2005) Phanerozoic geological evolution of Northern and Central Africa: an overview. J Afr Earth Sc 43:83–143
22. Youssef M (2003) Micropaleontological and Stratigraphical analyses of the Late Cretaceous/Early Tertiary Succession of the Southern Nile Valley (Egypt). Ph.D. Unpublished, Institut für Geologie, Mineralogie und Geophysik der Ruhr Universität Bochum, p 128
23. Ouda Kh, Aubry MP (2003) The upper–Paleocene–lower Eocene of the upper Nile Valley. Part 1, stratigraphy. In: Ouda, Kh and Aubry MP (eds) Paleocene–Eocene stratigraphy of the upper Nile Valley, part 1, Stratigraphy. Micropaleontology 49: 1–21
24. Said R (1961) Tectonic framework of Egypt and its influence on distribution of foraminifera. AAPG Bull 45:198–218
25. Said R, Sabry H (1964) Planktonic foraminifera from the type location of Esna Shale in Egypt. Micro-Paleontol 10:375–395. https://doi.org/10.2307/1484585
26. El Gammal RMH, Orabi HO (2019) Coniacian-late Campanian planktonic events in the Duwi formation, Red Sea region Egypt. J Geol Geophy 8(1):16
27. El-Naggar ZRM (1966) Stratigraphy and classification of type Esna Group of Egypt. Bull Am Assoc Petrol Geol 50:1455–1477
28. Dupuis C, Aubry MP, Steurbaut E, Berggren WA, Ouda Kh, Magioncalda R, Cramer B, Kent DV, Speijer RP, Heilmann-Clausen C (2003) The Dababiya Quarry Section: Lithostratigraphy, clay mineralogy, geochemistry, and paleontology. Micropaleontology 49:41–59
29. Aubry MP, Ouda K, Dupuis C, Berggren WA, Van Couvering JA, members of the working group on the Paleocene/Eocene Boundary (2007) Global Standard Stratotype-Section and Point (GSSP) for the base of the Eocene Series in the Dababiya Section (Egypt). Episodes 30:271–286
30. Berggren WA, Norris RD (1997) Biostratigraphy, phylogeny and systematics of Paleocene trochospiral planktic foraminifera. Micropaleontology 43:119
31. Olsson RK, Hemleben C, Berggren WA, Huber BT (1999) Atlas of Paleocene Planktonic foraminifera. Smithsonian Institution Press, Washington, D.C., p 252
32. Wade BS, Pearson PN, Berggren WA, Pälike H (2011) Review and revision of Cenozoic tropical planktonic foraminiferal biostratigraphy and calibration to the geomagnetic polarity and astronomical time scale. Earth Sci Rev 104(1–3):111–142. https://doi.org/10.1016/j.earscirev.2010.09.003
33. Gibson TG (1989) Planktonic: benthonic foraminiferal ratios: modern patterns and Tertiary applicability. Mar Micropaleontol 15:29–52
34. Sprong J, Kouwenhoven TJ, Bornemann A, Dupuis C, Speijer RP, Stassen P, Steurbaut E (2013) In search of the Latest Danian Event in a paleobathymetric transect off Kasserine Island, north-central Tunisia. Palaeogeogr Palaeoclimatol Palaeoecol 379–380:1–16
35. Berggren, W.A., Kent, D.V., Swisher, C.C., Aubry, M.P., 1995. A revised Cenozoic geochronology and chronostratigraphy. In: Berggren, W.A., Kent, D.V., and Hardenbol, J. (Eds.), Geochronology, time scales and global stratigraphic correlations: a unified temporal framework for a historical geology. Society of Economic Paleontologists and Mineralogists Special Publication. 54: 129–212
36. Berggren WA, Pearson PN (2005) A revised tropical and subtropical Paleogene planktonic foraminiferal zonation. J Foramin Res 35:279–298
37. Kaiho K, Hasegawa T (1994) End-Cenomanian benthic foraminiferal extinction and oceanic dysoxic events in the northwestern Pacific Ocean. Palaeogeogr Palaeoclimatol Palaeoecol 111:29–43
38. Jorissen FJ, De Stigter HC, Widmark JGV (1995) A conceptual model explaining benthic foraminiferal microhabitats. Mar Micropaleontol 26:3–15
39. Coccioni R, Galeotti S (1993) Orbitally induced cycles in benthonic foraminifera1 morphogroups and trophic structure distribution patterns from the Late Albian 'Amadeus Segment' (Central Italy). J Micropaleontol 12:221–239

40. Friedrich O, Reichelt K, Herrle JO, Lehmann J, Pross J, Hemleben C (2003) Formation of the Late Aptian Niveau Fallot black shales in the Vocontian Basin (SE France): evidence from foraminifera, palynomorphs, and stable isotopes. Mar Micropaleontol 49:65–85
41. Kaiho K (1994) Planktonic and benthic foraminiferal extinction events during the last 100 m.y. Palaeogeogr Palaeoclimatol Palaeoecol 111:45–71
42. Murray JW (2000) When Does Environmental Variability Become Environmental Change? The Proxy Record of Benthic Foraminifera. In: Martin RE (ed) Environmental micropaleontology: the application of microfossils to environmental geology, topics in geobiology, 15. Plenum Press, New York, pp 7–37
43. Mendes I, Gonzalez R, Dias JM, Lobo F, Martins V (2004) Factors influencing recent benthic foraminifera distribution on the Guadiana Shelf Southwestern Iberia. Mar Micropaleontol 51:171–192. https://doi.org/10.1016/j.marmicro.2003.11.001
44. Olsson RK, Nyong EE (1984) A paleoslope model for Campanian-lower Maastrichtian foraminifera of New Jersey and Delaware. J Foramin Res 14:50–69
45. Nagy, J., Kaminski, M.A., Kuhnt, W., Bremer, M.A., 2000. Agglutinated foraminifera from neritic to bathyal facies in the Palaeogene of Spitsbergen and the Barents Sea. In: Hart MB, Kaminski MA (Eds) Proceedings of the Fifth International Workshop on Agglutinated Foraminifera, vol 7. Grzybowski Foundation special publication pp 333–361
46. Nagy LG, Petkovits T, Kovács GM, Voigt K, Vágvölgyi C, Papp T (2011) Where is the unseen fungal diversity hidden? A study of *Mortierella* reveals a large contribution of reference collections to the identification of fungal environmental sequences. New Phytol 191:789–794. https://doi.org/10.1111/j.1469-8137.2011.03707.x
47. Polski W (1959) Foraminiferal biofacies off North Asiatic Coast. J Paleontol 33:569–587
48. Bandy L, Arnal E (1960) Concepts in foraminiferal paleoecology. Bull Am Assoc Pet Geol 44(12):1921–1932
49. Saint-Marc P (1986) Qualitative and quantitative analysis of benthonic foraminifers in Paleicene deep-sea sediments of the Sierra Leone Rise, central Atlantic. J Foraminifera Res 16(3):244–253
50. Kaiho K (1991) Global changes of Paleogene aerobic=anaerobic benthic foraminifera and deep-sea circulation. Palaeogeogr Palaeoclimatolol Palaeoecol 83:65–85
51. Corliss BH (1985) Microhabitats of benthic foraminifera within deep-sea sediments. Nature 314:435. https://doi.org/10.1038/314435a0
52. Bernhard JM (1986) Characteristic assemblages and morphologies of benthic foraminifera from anoxic, organic-rich deposits; Jurassic through Holocene. J Foraminifera Res 16:207–215. https://doi.org/10.2113/gsjfr.16.3.207
53. van Morkhoven FPCM, Berggren WA, Edwards AS et al (1986) Cenozoic cosmopolitan deep-water benthic foraminifera. Bull Cent Rech Explor 11:419–487
54. Alegret L, Arenillas I, Arz JA, Molina E (2001) Reconstruccio´n paleoambiental del tra´nsito Creta´cico – Terciario en La Lajilla (Me´xico) con foramını´feros. Geogaceta 30:19–21
55. Alegret L, Molina E, Thomas E (2003) Benthic foraminiferal turnover across the Cretaceous/Tertiary boundary at Agost (southeastern Spain): paleoenvironmental inferences. Mar Micropaleontol 48:251–279
56. Berggren WA, Aubert J (1975) Paleocene benthonic foraminiferal biostratigraphy, paleobiogeography and paleoecology of Atlantic-Tethyan regions: midway–type fauna. Palaeogeogr Palaeoclimatol Palaeoecol 18:73–192
57. Plummer HJ (1927) Foraminifera of the midway formation in Texas. Univ Texas Bull 2644(1926):1–206
58. Kellough GR (1965) Paleoecology of the foraminiferida of the wills point fonnation (Midway Group) in northeast Texas. Gulf Coast Assoc Geol Soc Trans 15:73–153
59. LeRoy LW (1953) Biostratigraphy of the Maqfi section Egypt. Geol Soc Am Mem 54:73
60. Lüger P (1985) Stratigraphie der marinen Oberkreide und des Alttertiärs im südwestlichen Obernil-Becken (SW-Ägypten) under besonderer Berücksichtigung der Mikropaläontologie, Palkologie und Paläogeographie. Berl Geowiss Abh A (Geol. Paläontol.) 63
61. Cushman JA (1925) Some new foraminifera from the Velasco Shale of Mexico Cushman Lab. Foram Res Contr I(1):18–23
62. Cushman JA (1926) The foraminifera of the Velasco Shale of the Tampico Embayment. Arner Assoc Petro Geo Bull 10:581–612
63. Saint-Marc P, Berggren WA (1988) A quantitative analysis of Paleocene benthic foraminiferal assemblages in central Tunisia. J Foraminifer Res 18:97–113
64. Schnack K (2000) Biostratigraphic und fazielle Entwicklung in der Oberkreide und im Alttertiar im Bereich der Kharga Schwelle, Westliche Wüste, SW € Agypten. Universitat Bremen, Berichte Fachbereich Geowissenschaften, p 151
65. Murray JW (1991) Ecology and palaeoecology of benthic foraminifera. Harlow: Longman Scientific and Technical, p 397
66. Podobina VM (1975) Foraminifera of Upper Cretaceous and Paleogene of the western Siberian Lowlands and their significance for stratigraphy. Tomsk University Publishing House. p 220
67. Boersma A, Shackleton NJ, Hall MA, Given QC (1979) Carbon and oxygen isotope records at DSDP Site 384 (North Atlantic) and some Paleogene paleotemperatures and carbon isotope variations in the Atlantic Ocean. Init Rep DSDP 43:695–717
68. Hewaidy AA, Cherif OH (1984) Contribution to the bathymetric variations of the Late Cretaceous Sea over the Abu Tartur area by using Foraminifera. Annals Geol Surv Egypt 15:231–241
69. Nagy J, Reolid M, Rodríguez-Tovar FJ (2009) Foraminiferal morphogroups in dysoxic shelf deposits from the Jurassic of Spitsbergen. Polar Res 28:1–8
70. Hawkes AD, Kemp AC, Donnelly JP, Horton BP, Peltier WR, Cahill N, Hill DF, Ashe E, Alexander CR (2016) Relative sea-level change in northeastern Florida (USA) during the last ~8.0 ka. Quaternary Sci Rev 142:90–101. https://doi.org/10.1016/j.quascirev.2016.04.016
71. Chen H, Shaw TA, Wang J, Engelhart SE, Nikitina D, Pilarczyk JE, Horton BP (2020) Salt-marsh foraminiferal distributions from mainland northern Georgia, USA: an assessment of their viability for sea-level studies. Open Quat 6(1):1–19. https://doi.org/10.5334/oq.80
72. Nagy J, Løfaldli M, Backstrom SA (1988) Aspects of foraminiferal distribution and depositional conditions in Middle Jurassic to Early Cretaceous shales in eastern Spits Bergen. In: Rogl F, Gradstein FM (eds) Second workshop agglutinated foraminifera, 30. Abhandlungen der geologischen Bundesanstalt, Wien, pp 287–300
73. Nagy, J., Pilskog, B., Wilhelmsen, R., (1990) Facies controlled distribution of foraminifera in the Jurassic North Sea Basin. In: Hemleben, C., et al. (Eds.), Paleoecology, Biostratigraphy, Paleoceanography and Taxonomy of Agglutinated Foraminifera. NATO ASI Series C327. Kluwer Academic Publishers, 621–657
74. Hull PM, Norris RD (2011) Diverse patterns of ocean export productivity change across the Cretaceous-Paleogene boundary: new insights from biogenic barium. Paleoceanography 26(3):3205. https://doi.org/10.1029/2010pa002082
75. Kaminski, M.A., Gradstein, F.M., (2005) Atlas of Paleogene Cosmopolitan Deep-Water Agglutinated Foraminifera. Krakow, Poland: Grzybowski Foundation
76. Kuhnt, W., Kaminski, M.A. (1996) The response of benthic foraminifera to the K/T boundary event—a review. In: Jardine, S., De Klasz, I., Debenay, JP, (eds), Geologie de l'Afrique et de l'Atlantique Sud-Compte-rendu des colloques de geologie

d'Angiers. Bull. Centres Rech. Explor.-Production Elf Aquitaine, Memoire, 16: 433–442
77. Arreguín-Rodríguez GJ, Barnet JS, Leng MJ, Littler K, Kroon D, Schmidt DN, Alegret L (2021) Benthic foraminiferal turnover across the Dan-C2 event in the eastern South Atlantic Ocean (ODP Site 1262). Palaeogeogr Palaeoclimatol Palaeoecol 572:110410
78. Kelly DC, Arnold AJ, Parker WC (1999) The influence of heterochrony on the stratigraphic occurrence of *Morozovella angulata*. J Foramin Res 29(1):58–68
79. Quillévéré F, Aubry MP, Norris RD, Berggren WA (2002) Paleocene oceanography of the eastern subtropical Indian Ocean—an integrated magneto biostratigraphic and stable isotope study of ODP Hole 761B (Wombat Plateau). Palaeogeogr Palaeoclimatol Palaeoecol 184(3–4):371–405
80. Guasti E (2005) Early Paleogene environmental turnover in the southern Tethys as recorded by foraminiferal and organic-walled dinoflagellate cyst assemblages. University of Bremen, Bremen
81. Guasti E, Speijer RP, Brinkhuis H, Smit J, Steurbaut E (2006) Paleoenvironmental change at the Danian-Selandian transition in Tunisia: Foraminifera, organic-walled dinoflagellate cyst and calcareous nannofossil records. Mar Micropaleontol 59(3–4):210–229. https://doi.org/10.1016/j.marmicro.2006.02.008
82. Norris RD (1996) Symbiosis as an evolutionary innovation in the radiation of Paleocene planktic foraminifera. Paleobiology 22:461–480
83. Sprong J, Speijer RP, Steurbaut E (2009) Biostratigraphy of the Danian/Selandian transition in the southern Tethys. Special reference to the Lowest Occurrence of planktic foraminifera Igorina albeari. Geologica Acta 7(1–2):63–77. https://doi.org/10.1344/105.000000271
84. Soldan DM, Petrizzo MR, Silva IP, Cau A (2011) Phylogenetic relationships and evolutionary history of the paleogene genus igorina through parsimony analysis. J Foraminifer Res 41(3):260–84
85. Bornemann A, Jehle S, Lägel F, Deprez A, Petrizzo MR, Speijer RP (2021) Planktic foraminiferal response to an early Paleocene transient warming event and biostratigraphic implications. Int J Earth Sci 110(2):583–594. https://doi.org/10.1007/s00531-020-01972-z
86. Jennions SM, Thomas E, Schmidt DN, Lunt D, Ridgwell A (2015) Changes in benthic ecosystems and ocean circulation in the Southeast Atlantic across Eocene Thermal 916 Maximum 2. Paleoceanography 30:1059–1077. https://doi.org/10.1002/2015PA002821
87. Thomas E, Boscolo-Galazzo F, Balestra B, Monechi S, Donner B, Röhl U (2018) Early Eocene thermal maximum 3: biotic response at walvis ridge (SE Atlantic Ocean). Paleoceanogr Paleoclimatol 33(8):862–883. https://doi.org/10.1029/2018PA003375
88. Griffith EM, Thomas E, Lewis AR, Penman DE, Westerhold T, Winguth AME (2021) Bentho-pelagic decoupling: the marine biological carbon pump during eocene hyperthermals. Paleoceanogr Paleoclimatol 36:e2020PA004053
89. Steurbaut E, Sztrakos K (2008) Danian/Selandian boundary criteria and North Sea Basin-Tethys correlations based on calcareous nannofossil and foraminiferal trends in SW France. Mar Micropaleontol 67(1–2):1–29. https://doi.org/10.1016/j.marmicro.2007.08.004
90. Canudo JI, Molina E (1992) Planktic foraminiferal faunal turnover and bio-chronostratigraphy of the Paleocene-Eocene boundary at Zumaya (northern Spain). Rev Soc Geol Esp 5:145–157
91. Geological map of Egypt (1981) Geological survey of Egypt and mining authority. Cario Scale 1:1000000